EFFECT OF INCREASED VOLUME OF FIBERS ON THE FRACTURE PROPERTIES OF CEMENTITIOUS COMPOSITES

A THESIS SUBMITTED TO
THE GRADUATE SCHOOL OF NATURAL AND APPLIED SCIENCES
OF
MIDDLE EAST TECHNICAL UNIVERSITY

BY

UFUK EMRE ALTÜRK

IN PARTIAL FULFILLMENT OF THE REQUIREMENTS
FOR
THE DEGREE OF MASTER OF SCIENCE
IN
CIVIL ENGINEERING

SEPTEMBER 2019

Approval of the thesis:

EFFECT OF INCREASED VOLUME OF FIBERS ON THE FRACTURE PROPERTIES OF CEMENTITIOUS COMPOSITES

submitted by **UFUK EMRE ALTÜRK** in partial fulfillment of the requirements for the degree of **Master of Science in Civil Engineering Department, Middle East Technical University** by,

Prof. Dr. Halil Kalıpçılar
Dean, Graduate School of **Natural and Applied Sciences** _____

Prof. Dr. Ahmet Türer
Head of Department, **Civil Engineering** _____

Prof. Dr. İsmail Özgür Yaman
Supervisor, **Civil Engineering, METU** _____

Dr. Burhan Aleessa Alam
Co-Supervisor, **Civil Engineering, METU** _____

Examining Committee Members:

Prof. Dr. Barış Binici
Civil Engineering, METU _____

Prof. Dr. İsmail Özgür Yaman
Civil Engineering, METU _____

Assoc. Prof. Dr. Serdar Göktepe
Civil Engineering, METU _____

Assist. Prof. Dr. Can Baran Aktaş
Civil Engineering, TEDU _____

Assist. Prof. Dr. Alper Aldemir
Civil Engineering, Hacettepe University _____

Date: 10.09.2019

I hereby declare that all information in this document has been obtained and presented in accordance with academic rules and ethical conduct. I also declare that, as required by these rules and conduct, I have fully cited and referenced all material and results that are not original to this work.

Name, Surname: Ufuk Emre Altürk

Signature:

ABSTRACT

EFFECT OF INCREASED VOLUME OF FIBERS ON THE FRACTURE PROPERTIES OF CEMENTITIOUS COMPOSITES

Altürk, Ufuk Emre
Master of Science, Civil Engineering
Supervisor: Prof. Dr. İsmail Özgür Yaman
Co-Supervisor: Dr. Burhan Aleessa Alam

September 2019, 78 pages

To apply fiber as a reinforcement, which is much older than the history of concrete, together with concrete is rather a new technology, while cement based products are the most consumed materials after water, considering the consumption amounts. The application areas of fiber reinforced concrete are growing day by day. However, in common practice, fiber content is usually limited up to 2% due to economical, workability and agglomeration problems.

This study investigates the changes in the performance of nine FRC mixes built with three different types of fibers; steel, polypropylene and polypropylene-polyethylene copolymer, with three different dosages; 2%, 4% and 6% per volume. With the help of fly ash and concrete chemicals, the properties of the matrix can be regulated to breach the limit amount of fibers, provided to act as single body. To measure the increase in the flexural capacity and energy absorption rates, and also any effects on the compressive strength, three different test set-ups were prepared, cube compression, beam bending and tensile splitting tests. For data acquisition, video extensometer cameras are used. By the help of this high-frequency gadgets, each phase of fraction was recorded in detail. Energy absorption capacities were derived through

calculations with load and deflection data. To assure objective comparison, calculated energy values were used in the comparative study.

Keywords: FRC, Beam Bending Test, Tensile Splitting Test, Video Extensometer, Energy Absorption Capacity

ÖZ

ÇİMENTO ESASLI KOMPOZİT MALZEMELERDE YÜKSEK MİKTARDA LİF KULLANIMININ KIRILMA ÖZELLİKLERİ ÜZERİNDEKİ ETKİLERİ

Altürk, Ufuk Emre
Yüksek Lisans, İnşaat Mühendisliği
Tez Danışmanı: Prof. Dr. İsmail Özgür Yaman
Ortak Tez Danışmanı: Dr. Burhan Aleessa Alam

Eylül 2019, 78 sayfa

Tüketim miktarları göz önüne alındığında, sudan sonra en çok tüketilen malzemenin çimento tabanlı ürünler olduğu günümüzde, betonun geçmişine nazaran çok daha eski bir uygulama olan lif donatının betonla birlikte uygulanması görece yeni bir teknolojidir. Lif takviyeli beton uygulama alanları günden güne artmaktadır. Buna rağmen, yaygın uygulamada, maliyet, işlenebilirlik ve topaklanma sorunları nedeniyle lif içeriği genellikle %2 ile sınırlandırılır. Bu çalışmada, üç farklı dozajda (hacmen %2, %4 ve %6), üç farklı tipte lifle (çelik, polietilen ve polietilen-polipropilen kopolimer) oluşturulan dokuz lif takviyeli beton numunesinin performansındaki değişimler araştırılmaktadır. Uçucu kül ve beton kimyasalları marifetiyle, harcın özellikleri, liflerin sınır miktarını aşacak şekilde düzenlenerek, yekvücut davranışı sağlanabilmektedir. Eğilme kapasitesi, enerji soğurma oranı ve ayrıca basınç dayanımı üzerindeki etkilerini ölçmek üzere üç farklı deney düzeneği hazırlanmıştır: küp basma, kiriş eğme ve çekmede yarma deneyleri. Veri toplamak için, video ekstensometre kameradan faydalanılmıştır. Bu yüksek frekanslı cihazların yardımıyla, kırılma sürecinin her aşaması detaylı olarak kayıt altına alınabilmektedir. Enerji soğurma kapasitesi değerleri, yük ve yer değiştirme verileri ile yapılan hesaplamalar sonucunda

elde edilmiştir. Objektif bir karşılaştırma sağlanması maksadıyla, karşılaştırmada hesaplanan enerji değerleri kullanılmıştır.

Anahtar Kelimeler: Lif Takviyeli Beton, Kiriş Eğilme Deneyi, Çekmede Yarma Deneyi, Video Ekstensometre, Enerji Soğurma Kapasitesi

To My Family

ACKNOWLEDGEMENTS

I would like to express my gratitude to my supervisor Prof.Dr. İsmail Özgür Yaman, who gave me the opportunity to do this research, for his valuable guidance and encouragement.

I wish to thank to my co-supervisor Dr. Burhan Aleessa Alam for his endless support, patience and energy.

I owe thanks to METU Materials of Construction Laboratory staff; Cuma Yıldırım and Sadık Karakaş.

Special thanks to my friends Alper Aldemir and Kerem Ar for their help and motivation.

My thanks go to my colleagues, for their helping hand through all the stages of this thesis.

And last but not least, I would like to thank to my family, for their never-ending support and patience.

TABLE OF CONTENTS

LIST OF TABLES

TABLES

LIST OF FIGURES

FIGURES

LIST OF ABBREVIATIONS

COD	:	Crack Opening Displacement
CMOD	:	Crack Mouth Opening Distance
FRC	:	Fiber Reinforced Concrete
PP	:	Polypropylene
SCM	:	Supplementary Cementitious Materials
SFRC	:	Steel Fiber Reinforced Concrete
UTM	:	Universal Testing Machine
W/CM	:	Water to Cementitious Material Ratio

LIST OF SYMBOLS

a	:	Depth of notch, mm
A_c	:	Compression cross-sectional area, mm^2
b	:	Width of beam specimen, mm
d	:	Depth of beam specimen, mm
d	:	Density, (kg/m^3)
D	:	Diameter of cylindrical specimen, mm
F	:	Maximum load at failure, N
f_c	:	Compressive strength, MPa (N/mm^2)
f_c'		Corrected compressive strength, MPa (N/mm^2)
f_t	:	Tensional strength, MPa (N/mm^2)
$f_{t,sp}$	:	Tensional strength in splitting, MPa (N/mm^2)
L	:	Length of specimen between supports, mm
Δ	:	Average
σ	:	Flexural strength, MPa (N/mm^2)

CHAPTER 1

INTRODUCTION

1.1. General

In construction industry, concrete is mainly used to handle compressive stresses thanks to its beneficial mechanical properties. However, in case of tensile stresses, concrete needs to be "reinforced" to stay safe and sound. Using steel rebars as reinforcement is the traditional method applied to give concrete elements the ability to act against tensile and shear forces. Not to mention that these rebars provide ductility and increase the energy absorption capacity of the concrete element through the failing phase. As an alternative, adding fibers to concrete has been studied since 1960s (American Concrete Institute, 2002). When added to concrete, fibers that are made of different materials and types join up to form a randomly distributed skeleton throughout the matrix of the cement paste. In this manner, shrinkage cracks can be prevented and the load carrying capacities -both tensile and compressive- and toughness values can be increased to the desired level.

The properties of FRC (fiber reinforced concrete) depend on the properties of the cement paste as much as the characteristics of the fibers; like the type, shape, diameter, length, surface texture, etc. The tensile capacity of the FRC is related to the bonding strength between the cement paste and the fiber, and on the tensile strength of fiber itself. There are vast application areas of FRC in construction industry as non-structural, semistructural and structural elements. Shotcrete in tunneling, roads and pavements, concrete shell structures, precast elements, conventional load bearing structural elements, ballistic and explosion protection and even fire insulation are some examples for FRC applications (Li, 2002b). In most of the FRC applications, the fiber content is limited up to 2% for the cost and the workability concern. In the cases

where cost loses importance in order to satisfy specific needs, workability becomes the only obstacle for high dosage FRC. To overcome the workability obligation, SCMs (supplementary cementitious materials) can be utilized, like fly ash, which can improve the workability of fresh concrete, however a decrease in the early strength is inevitable (Tokyay, 2016).

1.2. Objectives and Scope

The aim of this work was to develop high-tensile-capacity FRC mixtures by increasing the fiber dosage way over the traditional uses, which is limited up to a range between 1% to 2%. Three different fiber types, two synthetic and one steel fiber, were used with dosages of 2%, 4% and 6% per volume. The mechanical properties of the concrete mixtures were investigated in terms of compressive strength, flexural strength, splitting tensile strength and energy absorption capacity values.

This thesis consists of five chapters including this one. The second chapter presents the evolution of technology and industry of fiber reinforced concrete throughout the time. The experimental methods used in this study are explained in detail in Chapter 3. In Chapter 4, the test results are declared and analyzed. Acquired information is evaluated through a “compare and contrast” process. Chapter 5, the final chapter, contains the conclusion of the whole study and some recommendations to the researchers for their forthcoming studies about this topic.

CHAPTER 2

FIBER REINFORCEMENT

2.1. Brief History of Fiber Usage in Construction Materials

Using fibers as reinforcement in construction materials dates back to 3,500 to 5,000 years ago; hay straws used in sunbaked bricks to improve material properties in ancient times (Brandt, 2008). Incorporating horsehair, hay straw, etc. in exterior plaster of mud is a traditional way of heat insulation applied to adobe structures in hot and dry climates. With the increase in consumption of concrete as an industrial material, in middle of the 19th century, to overcome the weakness against tensile agents, discrete fibers were tried, until Joseph Lambot introduced continuous wires to the concrete, leading today's conventional reinforcements (Neville, 1995). In early 1900s, cement-based pastes were reinforced with asbestos fibers with the Hatschek process (Bentur & Mindess, 2007). Due to its hazardous effects to human health, usage of asbestos was banned in 1950s. Subsequently, the studies about fiber reinforcement have taken place since the 1960s (American Concrete Institute, 2002).

However, the use of fibers was not as an alternative to the rebar reinforcement, but to enhance the performance of the brittle concrete based on the fracture mechanics of concrete (Zollo, 1997). Through all of those years different natural fibers, such as plant based, sisal, jute, bagasse, bamboo and animal hair (Bilba, Arsene, & Ouensanga, 2003; Mansur & Aziz, 1982; Onuaguluchi & Banthia, 2016; Savastano, Agopyan, Nolasco, & Pimentel, 1999; Sudin & Swamy, 2006), and artificial fibers, such as steel, glass, synthetic fibers, basalt and many others (Alnahhal & Aljidda, 2018; Bentur & Mindess, 2007; Betterman, Ouyang, & Shah, 1995; Chen, Gao, Geng, Zhang, & Liu, 2017; Mehta & Monteiro, 2006; Naaman, 1998; Shah & Naaman, 1976) have been developed and used by many researchers and manufacturers.

The advantages, that fiber reinforced concrete has over the traditional one, are mainly related to tensile properties. Although that fibers can improve the durability of concrete against shrinkage, freezing-thawing, chemical attacks and other terms (Aarthi & Arunachalam, 2018; Afroz, Patnaikuni, & Venkatesan, 2017; Ortega-López, Fuente-Alonso, Santamaría, San-José, & Aragón, 2018; Yousefieh, Joshaghani, Hajibandeh, & Shekarchi, 2017), what they offer in the name of making concrete a ductile material cannot be obtained by any other addition. Many studies through the years showed how fibers can help to increase the flexural strength (Pająk & Ponikiewski, 2013), shear strength (Soltanzadeh, Barros, & Santos, 2015), splitting tensile strength (Xu, Hao, & Li, 2012), direct tensile strength (Kim, Yoo, Kim, Shin, & Banthia, 2018) and impact resistance (Yoo & Banthia, 2017). For sure, none of those enhancements is perfectly obtained by only adding fibers, but by optimizing different factors such as the concrete strength (Abbass, Khan, & Mourad, 2018), concrete rheology (Grünewald, 2012), fiber type (Zhao, Yu, Geng, Jiang, & Liu, 2016), fiber shape (Bangi & Horiguchi, 2012) and fiber amount (Soufeiani et al., 2016). When all those factors are combined together in a proper way, a strong, durable, well-engineered ultra-performance fiber reinforced concrete composite can be obtained. Hence, the main advantage here is that this concrete will act as one composite and can have no need for extra reinforcements.

Few studies were performed to examine the effectiveness of replacing the steel rebars with fibers (Destree, 2004; Ding & Kusterle, 1999; Junker, Holschemacher, Müller, & Kieslich, 2017). On the other hand, in order to obtain such a super fiber reinforced concrete, the volume fraction of the fibers should be high enough to allow the fibers to act at any section of the concrete under any level of loading. However, this increase in the volume fraction affects adversely the workability of concrete, which might make it impossible to be pumped or even placed (Mehta & Monteiro, 2006). For that, the commercial fraction used is about 0.5% by volume, or 1% at most, and beyond that the workability might be completely lost. Yet, if the concrete matrix was designed

properly, a self-consolidating concrete with a fiber volume fraction of 2% can be reached (Li, 2002a). This show that the development of an ultimate fiber reinforced concrete must go through the fresh as well as the hardened properties of concrete. Flow tests and bleeding examination are enough for the fresh properties, but the hardened properties need more detailed tests. While the ultimate compressive strength might not change that much because of the fiber addition, the tensile strength and strain capacity are highly improved. This is because of the good post-cracking performance and the ability of the fiber reinforced concrete to show multiple cracks (Akkaya, Shah, & Ankenman, 2001; Tjiptobroto & Hansen, 1991).

To determine the tensile strength of the concrete there are different direct and indirect tests suggested by many standards and researchers. The direct tensile tests usually use specimens with reduced cross section in the region between the grip heads. This can be done by either using specimens with dog-bone shapes or making a large notch in the middle of the specimens (Alhussainy, Hasan, Rogic, Neaz Sheikh, & Hadi, 2016; Curosu, Mechtcherine, & Millon, 2016; Shin, Jang, Choi, & Lee, 2015). However, these kinds of specimens are not easy to be prepared and need special test setup and apparatus to apply the direct tension perfectly. For that, indirect tests became more popular to predict the tensile strength of concrete. Splitting tensile strength test can be considered as the most used one for indirect measurements, because it does not need an expensive setup and it is easy to be performed on either cylindrical or cubic specimens. Moreover, the main advantage of this test is that a big part of the concrete plane subjected to the fracture loads is under tensile stresses.

However, there are still some longitudinal stresses formed along the fracture plane, and the post-cracking behavior is not clearly obtained due to the unstable crack propagation, which can be considered as the main disadvantages of this test (Abrishambaf, Barros, & Cunha, 2015; Carmona & Aguado, 2012). In addition to this test, bending tests are also widely used for indirect tensile strength determination. This test can be performed in single point loading or third point loading conditions, where

the latter allows a larger region to be under uniform stresses. Moreover, direct shear tests can be the best judge when it comes to the use of fiber reinforced concrete as structural elements, since shear failure can be considered one of the most critical failures of concrete. Many methods and different tests can be performed in order to measure the shear performance (Bae, Chung, Choi, Jung, & Choi, 2018; Mostafazadeh & Abolmaali, 2016; Shadravan & Tehrani, 2017). Most of them are more than enough to represent the advantages of using fibers, especially for comparison reasons.

2.2. Fibers

Generally, dispersed, randomly oriented and discrete elements are called fibers (Tokyay, 2016). There are various ways to classify fiber materials according to their usage in the desired application (Bothma, 2013).

2.2.1. Types of Fibers

Fibers are generally grouped in two main classification: with respect to the forming material or to the geometry. The fiber types according to the material are shown in **Hata! Başvuru kaynağı bulunamadı.**. Moreover, mechanical properties of the fibers v ary according to the properties of their raw material. (Table 2.1)

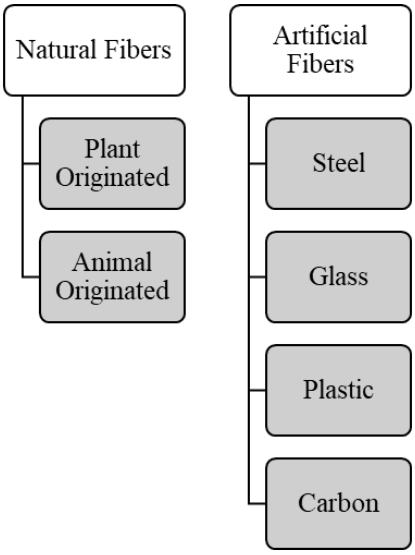

Figure 2.1. Types of Fiber Materials (Tokyay, 2016)

Table 2.1. *Properties of Various Fiber Types (Zollo, 1984)*

Material Type	Specific Gravity		Tensile Strength (MPa)		Elastic Modulus (GPa)	
Acrylic	1.16	1.18	296	1,000	14	19
Aramid I	1.44		2,930		62	
Aramid II	1.44		2,344		117	
Carbon I	1.9		1,724		380	
Carbon II	1.9		2,620		230	
Nylon	1.14		965		5	
Polyester	1.34	1.39	228	1,103	17	
Polyethylene	0.92	0.96	76	586	5	117
Polypropylene	0.9	0.91	138	690	3	5
Coconut	1.12	1.15	120	200	19	26
Sisal	-		276	568	13	26
Bagasse	1.2	1.3	184	290	15	19
Steel	7.8		1,000	3,000	200	
Glass	2.6		2,000	4,000	80	

* The color code for specific gravity is green for low and red for high, while for tensile strength and elastic modulus is red for low and green for high.

For the polymeric fibers, the diameter (D) is another distinction to classify as shown in **Hata! Başvuru kaynağı bulunamadı.**. With the fiber length (L), aspect ratio (L/D) c an be calculated. Workability of fresh concrete tends to decrease with the increment of fiber amount and aspect ratio of fibers (Soroushian & Bayasi, 1991).

Table 2.2. *Types of Polymeric Fibers According to EN 14889-2*

Type of Fiber	Dimensional Property
Class Ia: Micro Fibers	< 0.30 mm, Mono-Filamented
Class Ib: Micro Fibers	< 0.30 mm, Fibrillated
Class II: Macro Fibers	> 0.30 mm

2.2.2. Behavior of Fibers in Concrete

The manufacturing method and the final form of the fibers have a great role over the mechanical capacities. According to the morphology and crystalline structure of polymeric fibers of both melt-drawn and solid-state-drawn production (Figure 2.2**Hata! Başvuru kaynağı bulunamadı.**), if the bonding between the fiber and the cement paste is strong enough, the fiber tends to elongate along its axis (Steinmann, W.; Walter, S.; Beckers, M.; Seide, G.; Gries, 2013).

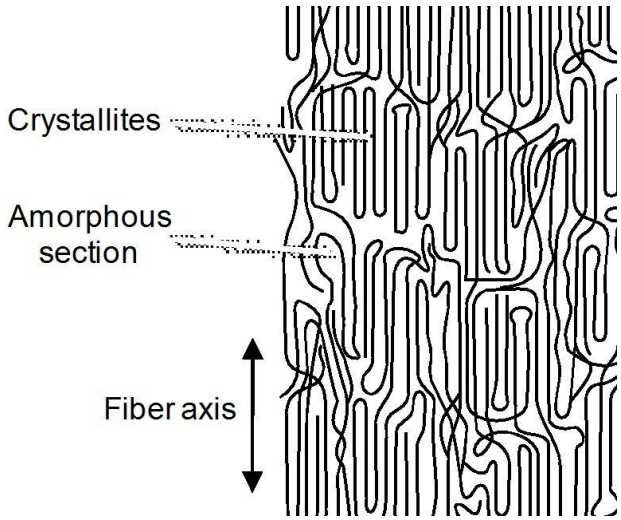

Figure 2.2. Model for Morphology of Polymeric Fibers (Steinmann, W.; Walter, S.; Beckers, M.; Seide, G.; Gries, 2013)

For steel fibers, the material has a larger deflection capacity thanks to its elasticity. For that, the bonding characteristics plays the main role. To increase the bonding, manufacturers produce fibers in deformed shapes. The commonly used forms are illustrated in Figure 2.3. In general, texture irregularities are kept on purpose to increase bonding between fibers and matrix.

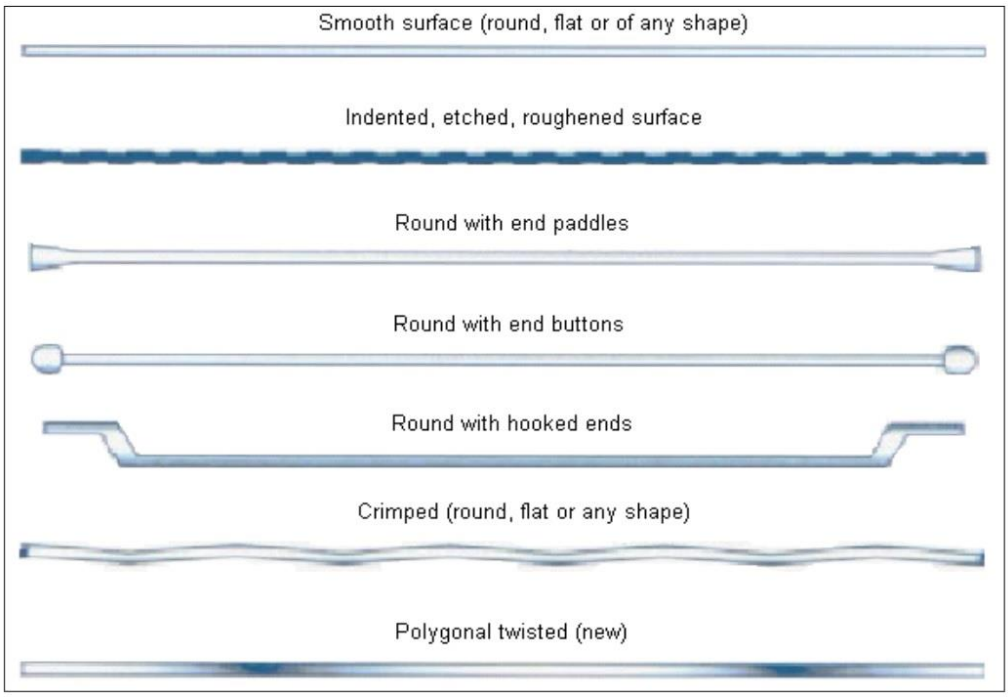

Figure 2.3. Steel Fiber Forms (Bothma, 2013)

In fresh state, fibers can be homogeneously mixed in the batch, then the whole mix is left to harden together. Although the hardened structure of FRC acts as a single body under various loading cases, with respect to the material properties of the fiber and the cement paste, stress concentrations may occur around the fiber filaments (Balaguru & Shah, 1992). Due to the random distribution of fibers, there is no alignment on the stress concentrations, resulting in an additional strain capacity. Therefore, fibers provide extra elasticity to the main body, and, the initial cracking deflection capacity of the paste is increased.

With the influence of excessive tensile forces, cracks occur throughout the cement matrix. At that moment, according to the load redistribution, fibers take the burden. Further increase in the load will lead to fiber failure. As stated in Figure 2.4, following the initial state (a), there are four main types of failure behavior of fibers in the post-cracking position: fiber pull-out (b), fiber failure (c), fiber bridging (d) and fiber/matrix debonding (e). A real-life failure observation can end up with a hybrid form of failure types mentioned above.

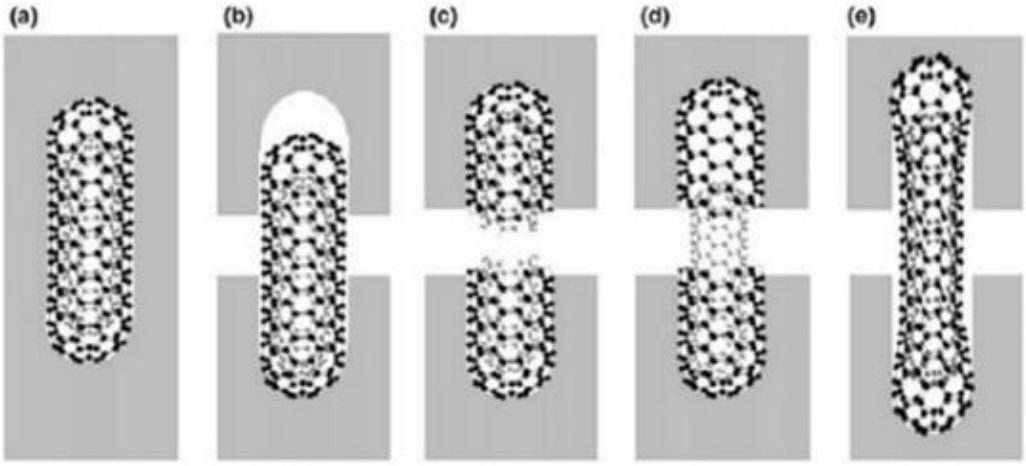

Figure 2.4. Fiber Failure Types (ETH Zurich, 2016)

The use of fibers changes also the crack propagation patterns. For plain concrete, a single crack initiates tensional and/or flexural loads concentration areas and this main crack widens as load increases whereas some smaller cracks may occur. In FRC case, after the first crack occurs, the body tends to crack at different points in directions parallel to the first crack with smaller width (Figure 2.5). Related to the fiber-matrix properties, a number of cracks may occur to restrain the propagation of the main crack, preserving the critical cross-section from disintegration (Mehta & Monteiro, 2006).

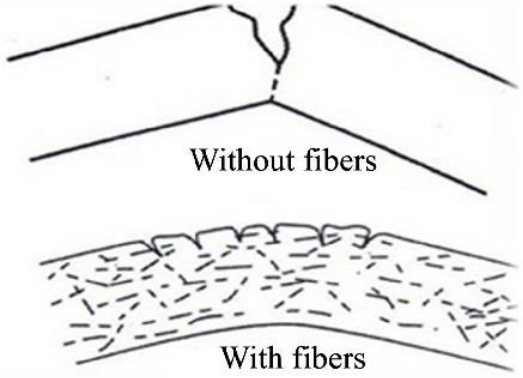

Figure 2.5. Increase in Flexure Toughness of Concrete with Fibers (Malhotra, 1980)

For plain concrete, the body breaks down when the ultimate flexural capacity is reached. However, in fiber-reinforced case, total load capacity is increased with deflection capacity and in the end, failure behavior becomes ductile, sudden failure does not occur which is presented in Figure 2.6 (Mehta & Monteiro, 2006).

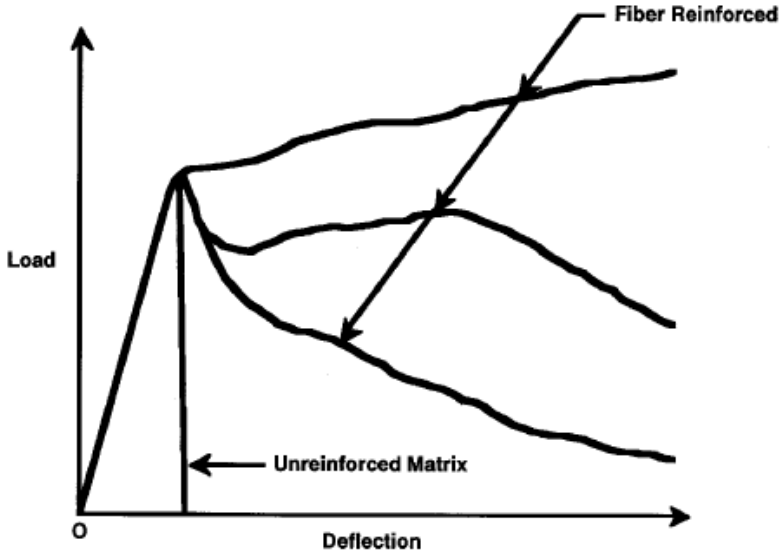

Figure 2.6. Load-Deflection Relation between Unreinforced Matrix and Fiber Reinforced Matrix (ACI Committee 544, 2002)

In the literature, fiber reinforcement in concrete/cementitious materials was studied in a wide range of perspectives: hybrid FRC of steel and PVA (polyvinyl alcohol) fibers

used in self-consolidating batch (Jen, Trono, & Ostertag, 2016); the response of SFRC (steel fiber reinforced concrete) beams under the effect of blast, impact and static loading conditions (J.-Y. Lee, Shin, Yoo, & Yoon, 2018); the effect of dosage and dimensions of steel fibers to fresh and hardened properties of FRC (Chu, Li, & Kwan, 2018), the influence of fiber content on the residual flexural strength of SFRC (J.-H. Lee, 2017), the mechanical and durability properties of hybrid FRC of steel and PP fibers (Afroughsabet & Ozbakkaloglu, 2015), the flexural response of SFRC with respect to strength of concrete, fiber content and strain rate (Yoo, Yoon, & Banthia, 2015), etc. The common point of all those researches was the upper limit for fiber content, it was limited up to 2% per volume. As an exception, 3% of fiber content was investigated to define the effect of strength and fiber content variation on dynamic properties of UHP (ultra-high performance)-FRC (Othman, Marzouk, & Sherif, 2019). In this thesis, the effect of fiber type and content was inspected, where 2%, 4% and 6% fiber ratios were used, contrary to the previous studies.

2.3. Test Methods to Define Properties of Fiber Reinforced Concrete

In engineering methodology, to define the properties of materials designed for the functionality and safety of structures, various tests and observations are carried on. To evaluate meaningful values, the test/observation procedures must be based on a scientifically logical pattern. Generally, after acquiring a satisfactory number of results, those procedures turned into the standards related to that topic. For FRC materials, there are some standard test methods used worldwide.

In this study, the tests carried out were focused on the hardened properties of FRC samples, to evaluate the performance of high fiber dosage addition. This is mainly because investigating the fresh properties of such mixtures requires an optimization study based on changing the mixture proportions. However, this study firstly aims to prove that such a high amount of fiber can be used in concrete, and secondly to

determine which dosage gives better performance. Improving the fresh properties is what should be done after this phase.

2.3.1. Compressive Strength Test

It is the most common test used to define the strength of hardened concrete samples. Both cylindrical and cubic samples can be prepared according to EN 12390-3. For cylindrical samples, compression surface preparations must be done, however for cubes, two opposite molded faces are enough to compress. In standard procedure, the samples are compressed at the age of 7 days and 28 days in a UTM (universal testing machine). It is assumed that in curing conditions, at 7 days 65% and at 28 days 99% of the ultimate compression capacity is reached, approximately. Load rate should be in between 0.2-1.0 MPa/s. Compressive strength can be determined as follows:

$$f_c = \frac{F}{A_c}$$

where;

f_c is compressive strength in MPa,

F is applied load in N,

A_c is compression cross-sectional area in mm^2.

2.3.2. Direct Tension Test

Although the main reason for adding fibers to concrete is to improve its tensile strength, no direct test for concrete elements can be found neither in EN nor in ASTM standards (Erdoğan & Erdoğan, 2014). This is mainly because concrete samples are too large and more fragile to be gripped by tensile test devices. However, some setups are derived from direct tension of ductile materials, e.g. concrete specimens cast in a dog-bone shape or have anchorage, are pulled from both ends. The main drawback of this type of tests is that the failure usually occurs at the grip points of the specimen. For that, alternative indirect tensile tests aim to use a loading pattern that will make

part of the concrete specimen subjected to tension and predict the tensile stresses based on that area and the corresponding loads.

Another way to define the tensile strength of concrete specimens is described in EN 1992-1-1; evaluation of tensile strength based on empirical calculations with the help of compressive strength. According to the code:

$$f_t = \begin{cases} 0.30 \times {f_c}^{(2/3)}, \leq C50/60 \\ 2.12 \times \ln\left(1 + \left(\frac{f_c}{10}\right)\right), > C50/60 \end{cases}$$

where;

f_t is tensional strength in MPa,

f_c is compressive strength in MPa.

2.3.3. Beam Bending Test

In this test procedure, a beam specimen is put over two supports under its ends and subjected to an increasing load acting on the top surface. This loading pattern make the lower half of the beam under tension forces. Considering the lowest midpoint of the beam, the acting tensile stress can be calculated based on the applied bending moment. This test has two commonly used setups as described below.

2.3.3.1. Single Point Bending Test

Test load is applied on the top midpoint of the support span (Figure 2.7). The load is increased in a planned pattern until a cracking failure or predetermined deflection is reached. EN 12390-5 and ASTM C 293 are the standard codes for this test procedure. The major drawback of this test is that there is a big chance that the crack would not occur under the midpoint of the beam, since there is a large possibility that the weakest section is not there. To determine the strength value, the following formula can be used:

$$\sigma = \frac{3FL}{2bd^2}$$

where;

σ is flexural strength in MPa,

F is applied load in N,

L is length of specimen between supports in mm,

b is width of beam specimen in mm,

d is depth of beam specimen in mm.

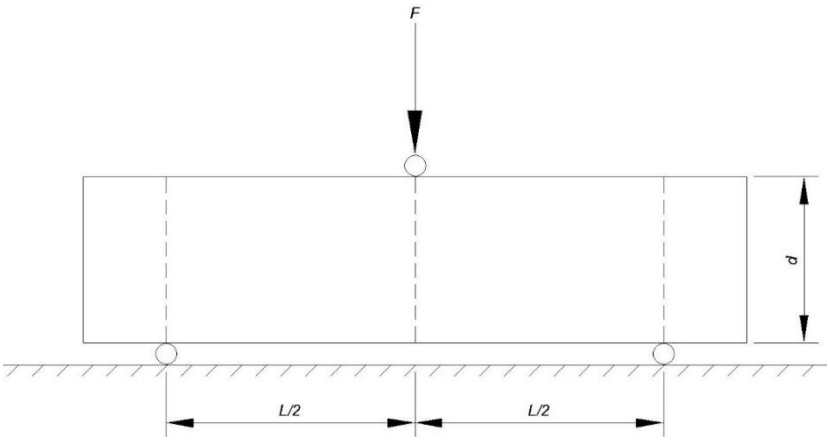

Figure 2.7. Single Point Bending Test Scheme

2.3.3.2. Third-Point Point Bending Test

The aim of this test is to overcome the drawback of the single point bending test and create a constant moment zone in the middle of beam by applying equal loads on two points (supports) at the top surface of the beam through a third point at the middle. The exact dimensions specified for this test varies between EN 12390-5 and ASTM C78 standards, however, in both, the length between the supports divided into three equal segments, and the loads applied on the dividing points (Figure 2.8). For the EN Code, the loading rate should be in between 0.04-0.06 MPa/s. Up to the initial cracking point, flexural strength of the specimen can be calculated as follows:

$$\sigma = \frac{FL}{bd^2}$$

where;

σ is flexural strength in MPa,

F is applied load in N,

L is length of specimen between supports in mm,

b is width of beam specimen in mm,

d is depth of beam specimen in mm.

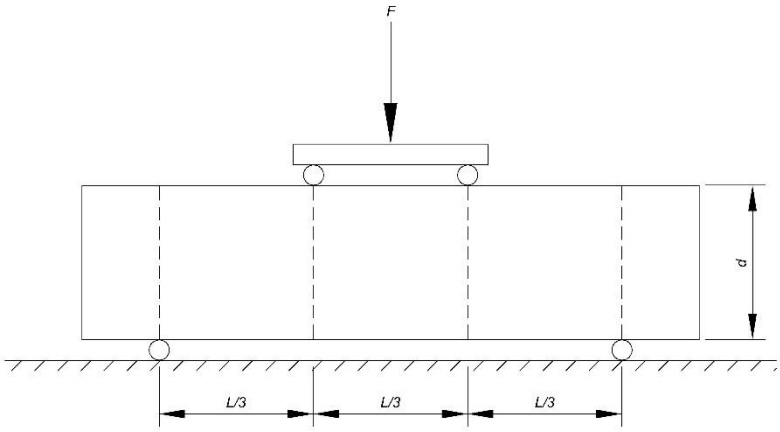

Figure 2.8. Third-Point Loading Test Scheme

2.3.4. Splitting Tensile Strength Test

In this test, a uniform continuous load is applied on a cylindrical specimen along its length at two ends of vertical diameter, as shown at Figure 2.9. A constant tensile force plane is created along the loaded diameter throughout the specimen towards its sides. EN 12390-6 and ASTM C 496 standards are used for the procedure stated above. For plain concrete, the splitting tensile strength is derived as follows:

$$f_{t,sp} = \frac{2F}{\pi DL}$$

where;

$f_{t,sp}$ is tensional strength in splitting in MPa,

F is applied load in N,

D is diameter of specimen in mm,

L is length of specimen between supports in mm.

Figure 2.9. Splitting Tensile Strength Test Setup

For plain concrete, according to the EN 1992-1-1 code, formulas of both flexural and splitting tensile strength with respect to the calculated direct tensile strength are as follows:

$$\sigma = \max\left\{\left(1.6 - \frac{d}{1000}\right) f_t; f_t\right\}$$

$$f_{t,sp} = 0.9 \times f_t$$

where;

σ is flexural strength in MPa,

$f_{t,sp}$ is tensional strength in splitting in MPa,

f_t is tensional strength in MPa.

2.3.5. Tests Used for Fiber Reinforced Concrete

While the tests described above were originally designed to indirectly determine the tensile strength of plain concrete, some modifications should be made to adapt these tests to fiber reinforced concrete. Considering that the fibers in the concrete matrix start to act after the initial cracks, the test evaluation should continue beyond the ultimate strength. In other words, since the fibers need the concrete to fail in order to start bridging the cracks, evaluating the FRC specimens should not focus on one point only (the ultimate strength) but examine the whole performance. For that, some test methods were modified to measure the strength at specific deflections, which will allow to compare mixtures made of different fiber types and amounts at those deflections. Another method used to evaluate the performance of FRC is to determine the toughness of the specimen, which is a relation combining the applied load and the occurred deformation at each point of the test.

2.3.5.1. Beam Bending Test (Single Point Bending with CMOD)

In the tests described previously, it is not possible to specify the exact point where the initial crack will occur. However, in this test, a notch, with a 25 mm depth and 5 mm width, is made at the middle of the beam specimen and the load is applied just at the same plane above the notch as shown in Figure 2.10. This will force the crack to occur at the end of this notch, hence the stress calculation will be more accurate. According to the test standard, EN 14845-2, the specimen must satisfy a residual strength of 1.5 MPa at 0.5 mm CMOD (crack mouth opening displacement) and 1 MPa at 3.5 mm CMOD. The strength values can be evaluated as follows:

$$\sigma = \frac{3FL}{2b(d-a)^2}$$

where;

σ is flexural strength in MPa,

F is applied load in N,

L is length of specimen between supports in mm,

b is width of beam specimen in mm,

d is depth of beam specimen in mm,

a is depth of notch in mm.

Figure 2.10. Single Point Loading, CMOD Test Setup

2.3.5.2. Flexural Performance of Fiber-Reinforced Concrete (Using Beam with Third-Point Loading) Test

An FRC beam of 350 × 100 × 100 mm^3 dimensions is subjected to third-point loading test with a span length of 300 mm in this test, ASTM C1609 (Figure 2.11). The aim of the test is to determine the first-peak and peak loads and the corresponding stresses for specific deflection values, L/600 and L/150, where L is the span length. The test also determines the toughness corresponding to the area under the load-deflection curves between 0 and L/150 deflections.

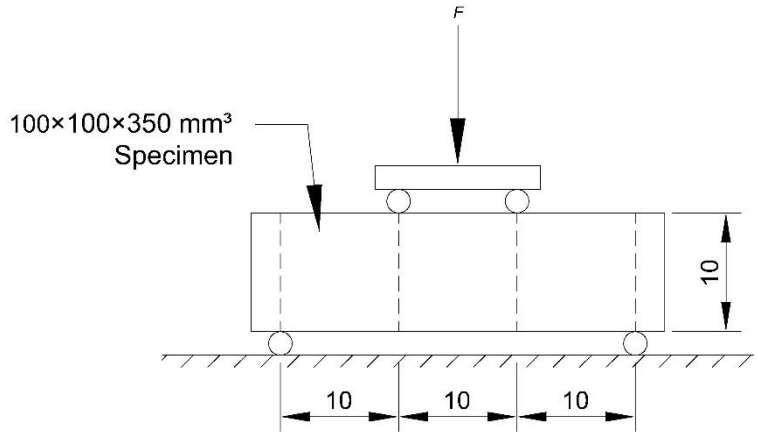

Figure 2.11. ASTM C1609 Test Setup

2.3.5.3. Average Residual-Strength of Fiber-Reinforced Concrete Test

This test method, known as ASTM C1399, is very similar to the previous one. Differently, this one consists of two phases. In the first phase, FRC beam of $350 \times 100 \times 100\ mm^3$ is placed over a steel plate as in third-point loading test as shown in Figure 2.12. By the help of the plate, a controlled cracking of the beam is provided. And in the second phase, initially cracked beam is further loaded to see the load-deflection relations (Banthia & Dubey, 1999). By this, the cracked concrete matrix will have no contribution to the toughness of the beam.

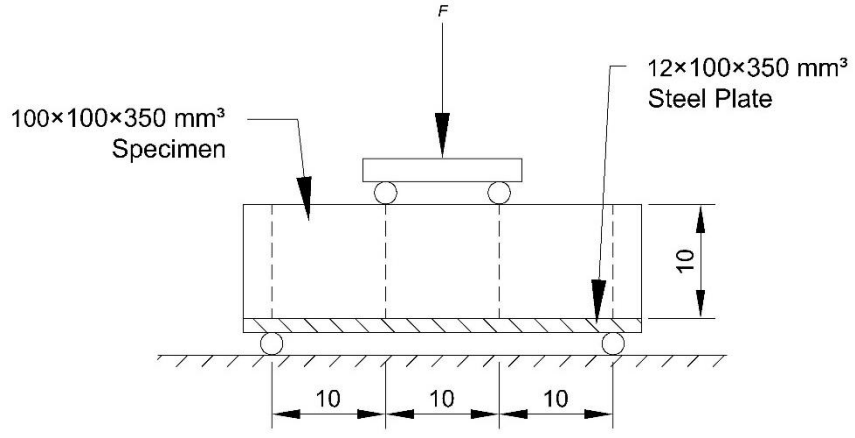

Figure 2.12. ASTM C1399 Test Setup

2.3.5.4. Average Residual-Strength of Fiber-Reinforced Concrete Test

In this test -ASTM C1550, a circular panel of 75 mm thickness and 800 mm diameter is loaded at the center, where the specimen is carried on three supports forming an equilateral triangle with the same center as shown in Figure 2.13. To provide single point loading and to prevent undesired load concentrations, load is applied by a hemispherical headed steel bar on the center point. Up to a defined deflection, loading values are determined to verify the flexural toughness capacity of the specimen (Hetemoğlu, 2018).

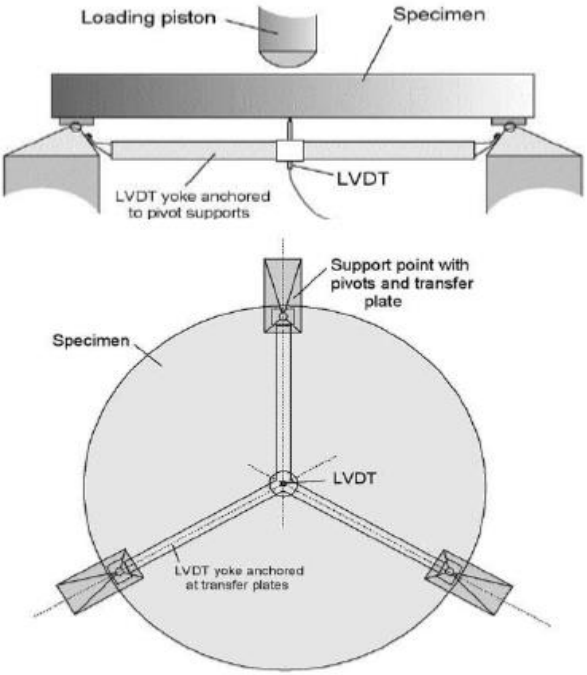

Figure 2.13. Centrally Loaded Round Panel Test (ASTM C 1550, 2012)

2.3.5.5. Double Punch (Barcelona) Test

Like splitting tensile test, Barcelona test is also an indirect tensile test. In this test, a cylindrical specimen with 15 cm height and 15 cm diameter is compressed on the axis passing through the centers of each circular surface with punched of 3.75 cm diameter. The failure mechanism is shown in Figure 2.14. Crack path, crack width and the

increase in the diameter of the specimen are measured (Molins, Aguado, & Saludes, 2009).

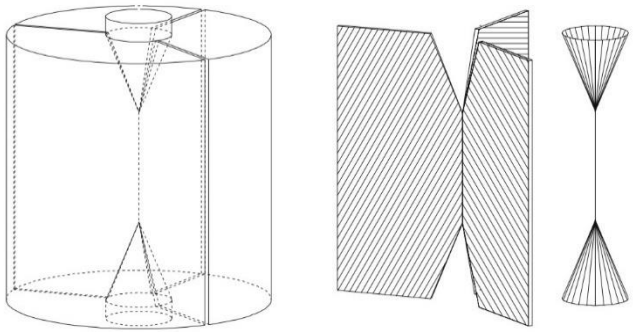

Figure 2.14. Failure Mechanism of Barcelona Test (Molins, Aguado, & Saludes, 2009)

CHAPTER 3

EXPERIMENTAL PROGRAM

3.1. General

After making some preliminary batches using a trial-and-error procedure, a base concrete mixture was defined to examine the mechanical properties of cementitious composites with high proportion of fibers. To enhance workability, homogeneity and binding properties of the batch, viscosity attributes were adjusted by the help of SCMs and chemical admixtures, but coarse aggregate was excluded for the same reason. By using two synthetic and one steel fibers with volume ratios of 2%, 4% and 6%, a total of nine FRC mixtures were prepared. After that, a combination of four tests, compression, bending and splitting tensile, was applied on the specimens after the age of 28 days.

3.2. Materials

3.2.1. Cement

CEM I 42.5 R type Portland cement (Baştaş Cement Company, Ankara) was used in specimen preparation. The chemical, physical and mechanical properties provided by the producing company are given in Table 3.1.

Table 3.1. *Properties of Cement*

Portland Cement CEM I 42,5 R Chemical Properties (%)	
CaO	63.71
SiO_2	18.53
Al_2O_3	4.60
Fe_2O_3	3.1
MgO	1.6
SO_3	3.05
K_2O	0.90
Na_2O	0.45
Cl	0.021
Loss on Ignition (LoI)	4.37
Insoluble Residue (IR)	0.76
Physical and Mechanical Properties	
Specific Gravity (g/cm^3)	3.11
Blaine Fineness (cm^2/g)	3411
Initial Setting (min)	165
Final Setting (min)	215
Compressing Strength (MPa)2 days	26.4
Compressing Strength (MPa) 7 days	37.5
Compressing Strength (MPa) 28 days	48.3

3.2.2. Fly Ash

Fly ash (Type F) obtained from Sugözü Thermal Power Plant was used as mineral admixture to improve the cementitious matrix. This type of fly ash was chosen due to its spherical grain shape, which enhances the workability in the plastic phase, allowing the addition of large amount of fibers, causing less voids, furthermore, affecting the durability and the strength of the final product accordingly.

3.2.3. Aggregate

Single sized (fine material) crushed limestone was used in the study. The physical properties and the sieve analysis related with the moisture content are given in Table 3.2 and Figure 3.1. Sieve Analysis of the Aggregate, respectively.

Table 3.2. *Physical Properties of Aggregate*

	Aggregate (Fine)
Dry Specific Gravity	2.58
SSD Specific Gravity	2.63
Apparent Specific Gravity	2.70
Water Absorption Capacity(%)	1.75%

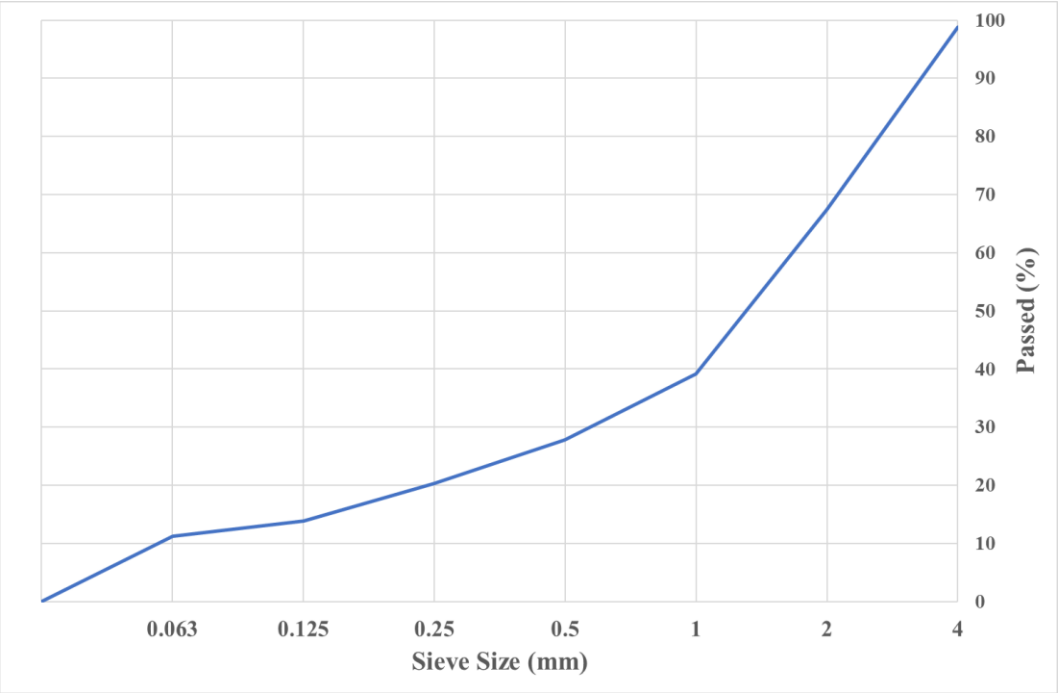

Figure 3.1. Sieve Analysis of the Aggregate

3.2.4. Chemical Admixtures

MasterGlenium 51 (polycarboxylate high range water reducer) was used to increase workability with less water and to prevent flocculation of the fibers.

3.2.5. Fibers

Three different types of fibers -BarChip 48, Forta Ferro and Dramix 4D- were added to the concrete mixes throughout the test procedure as shown in Figure 3.2 and their properties are listed in Table 3.3.

a. BarChip 48 b. Forta Ferro c. Dramix 4D

Figure 3.2. Types of Fibers

Table 3.3. *Properties of Types of Fibers*

	Barchip	Forta	Dramix
Commercial Name	BarChip 48	Forta Ferro	Dramix 4D
Base Material	Virgin Polypropylene	Pure Copolymer Polypropylene/ Polyethylene	Steel
Shape/Surface Texture	Rectangular-Embossed	Twisted Bundles	Curved 3 Times in Both Ends
Length (mm)	48	54	60
Diameter (mm)	0.72	0.34	1.05
Aspect Ratio	66.67	158.82	57.14
Number of Fibers per kg	59,500	220,000	2,313
Tensile Strength (MPa)	640	550-750	1,450
Young's Modulus (GPa)	12	5.75	20

3.3. Mix Design

In this study, nine diverse designs -three different fiber dosages (2%, 4% and 6% per volume) of three different fiber types (Barchip, Forta, Dramix)- were cast upon a control mix. The amount of the binder material was kept constant, while the amount of aggregate changed with the change in the fiber volume. W/CM (water to cementitious material ratio) was kept constant as 0.25 for the synthetic fibers and 0.21 for the steel fiber. The details of the mixtures are presented in Table 3.4. The water amount was reduced for SFRC specimens to achieve the same consistency because steel fibers were covered with a water-activated, lubricant wax.

Table 3.4. *Mix Design Proportions*

Specimen	Cement (kg/m^3)	Fly Ash (kg/m^3)	Water (kg/m^3)	SP (kg/m^3)	Fiber (kg/m^3)	Fine Ag. (kg/m^3)	Total W. (kg/m^3)	W/CM Ratio
Reference	400	400	200	8	0	1,256	2,264	0.25
Barchip-2	400	400	200	8	18.2	1,204	2,230	0.25
Barchip-4	400	400	200	8	36.4	1,152	2,196	0.25
Barchip-6	400	400	200	8	54.6	1,100	2,163	0.25
Forta-2	400	400	200	8	18.2	1,204	2,230	0.25
Forta-4	400	400	200	8	36.4	1,152	2,196	0.25
Forta-6	400	400	200	8	54.6	1,100	2,163	0.25
Dramix-2	400	400	170	8	159.6	1,204	2,342	0.21
Dramix-4	400	400	170	8	319.2	1,152	2,449	0.21
Dramix-6	400	400	170	8	478.8	1,100	2,557	0.21

3.4. Specimen Preparation

Initially, aggregates were placed in the drum of a rotary concrete mixer with one third of the water and mixed for two minutes (Figure 3.3). Right after, cement and fly ash were added, and the mixer was run for one minute. The superplasticizer initially

poured into the second third of the water and stirred to spread the solid particles homogenously into the whole batch. This water is added to the mixer and mixing continued for another two minutes, then, fibers were introduced. Finally, the rest of the water was added gradually, and the mixing process continued until a homogenous mixture is obtained.

Figure 3.3. Rotary Drum Concrete Mixer

The concrete was cast into the molds (150 mm cube molds for compressive strength, beam molds with dimensions of $600 \times 150 \times 150\ mm^3$ for bending tests and cylindrical molds with 100 mm in diameter and 200 mm in height for splitting tensile test) and kept for 24 hours, then removed out of the molds and kept under normal curing conditions for another 27 days. For each batch, 4 cubic, 3 beam and 2 cylindrical specimens were prepared with an approximate concrete volume of 0.06 m^3 in total.

3.5. Tests and Measurement

All the specimens were measured in dimension and weight to define the density of the final product. The FRC density gives an idea about the homogeneity of compaction

and the existence of any undesired porous formations in the specimens. As stated at Table 3.5, increasing fiber content tends to decrease the bulk density by drawing entrapped air into the specimen through flocculation.

Table 3.5. *Density Values of Specimens*

Fiber Type	Fiber Content (%)	Δd (kg/m^3)		
		Cube	Beam	Cylinder
Reference	-	2,285	2,277	2,297
Barchip	2	2,258	2,291	2,251
	4	2,221	2,247	2,152
	6	2,210	2,232	2,165
Forta	2	2,232	2,219	2,197
	4	2,206	2,227	2,126
	6	2,128	2,107	2,026
Dramix	2	2,421	2,401	2,361
	4	2,397	2,544	2,377
	6	2,579	2,709	2,580

3.5.1. Compression Tests

This test was carried on 150 mm cubic specimens in two different modes. The first one is the traditional force control compressive test used to determine the ultimate compressive strength. The test was performed using a universal testing machine, Figure 3.4.a, with a load rate of 13.5 kN/s. The ultimate force was only recorded out of this test. As for the second compressive test, a displacement control test with a load rate of 1 mm/s was applied on cube specimens using a different testing machine, Figure 3.4.b. The load-displacement curves were obtained out of this test to examine the behavior of the fiber reinforced concrete under direct compression.

a. Load Control

b. Displacement Control

Figure 3.4. Compression Test Devices

3.5.2. Bending Tests

This test was performed on beam specimens with dimensions of $600 \times 150 \times 150$ mm^3. This size was chosen to make use of full length of the fibers. A notched specimen was not preferred for two main reasons. The first one is to allow multiple cracks to occur, and the second one is the difficulty of cutting the notch with such amount of fibers. The tests were carried out using a servohydraulic universal testing machine, MTS trademark, with a 250 kN load and a 200 mm stroke capacity. A deformation-controlled test under static loading rate of 1 mm/s was performed on the beam specimens. All the tests were applied through third point bending test setup (Figure 3.5). During the tests applied load data were obtained using a load cell mounted on the upper part of the bending fixture. The load-displacement and energy-displacement curves were obtained out of this test.

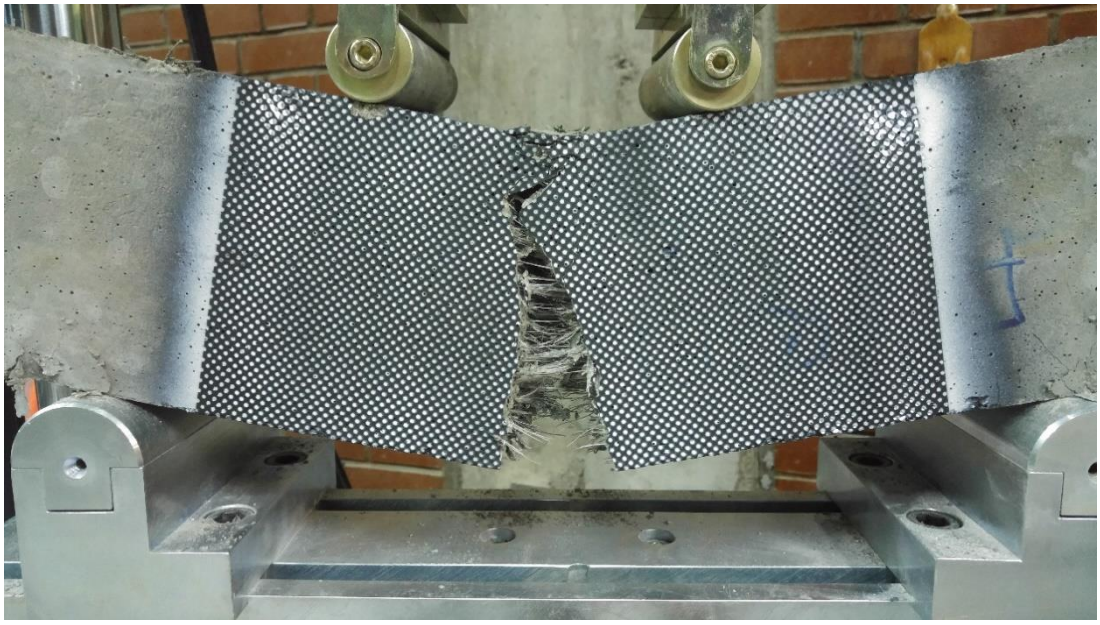

Figure 3.5. Bending Test

3.5.3. Splitting Tensile Strength Tests

This test was used as an indirect tensile test method, in order to define tensile characteristics of FRC element instead of direct tension test, to avoid undesired cracks caused by stress concentrations near grips. However, in this study, this test was performed under displacement control mode, with a load rate of 1 mm/s, to be able to examine the full effect of fibers under this type of tests. Cylindrical samples with diameter of 100 mm and height of 100 mm were used in this test. The reason for using this small height is to not exceed the capacity of the testing machine. Load-crack width curves were obtained for this test. The crack width was measured between two points on the middle horizontal axis of the specimen, using a video extensometer, Figure 3.6.

Figure 3.6. Splitting Tensile Strength Test

CHAPTER 4

RESULTS AND COMPARISON

4.1. Compression Tests

The ultimate compressive strength test results of load-controlled compression tests are listed in Table 4.1 and Figure 4.1. Moreover, data of displacement-controlled compression tests are presented in Table 4.2.

Based on the test results, the effect of the fiber type on the compressive strength can be clearly seen through the huge improvement when steel fibers were used. In addition to that, the effect of using high fiber dosage on preventing or delaying the complete failure of the specimens under compression is obvious. This positive effect increases with the increase in fiber amount, and it is higher when steel fibers are used.

Table 4.1. *Compression Test Results (Load-Controlled)*

Fiber Type	Fiber Content (%)	f_c' (MPa)*
Plain Control	-	53.27
Barchip	2	71.09
	4	60.11
	6	59.35
Forta	2	59.23
	4	51.46
	6	43.54
Dramix	2	75.72
	4	80.14
	6	74.86

* Compressive strength values were corrected with respect to the actual compression surface area.

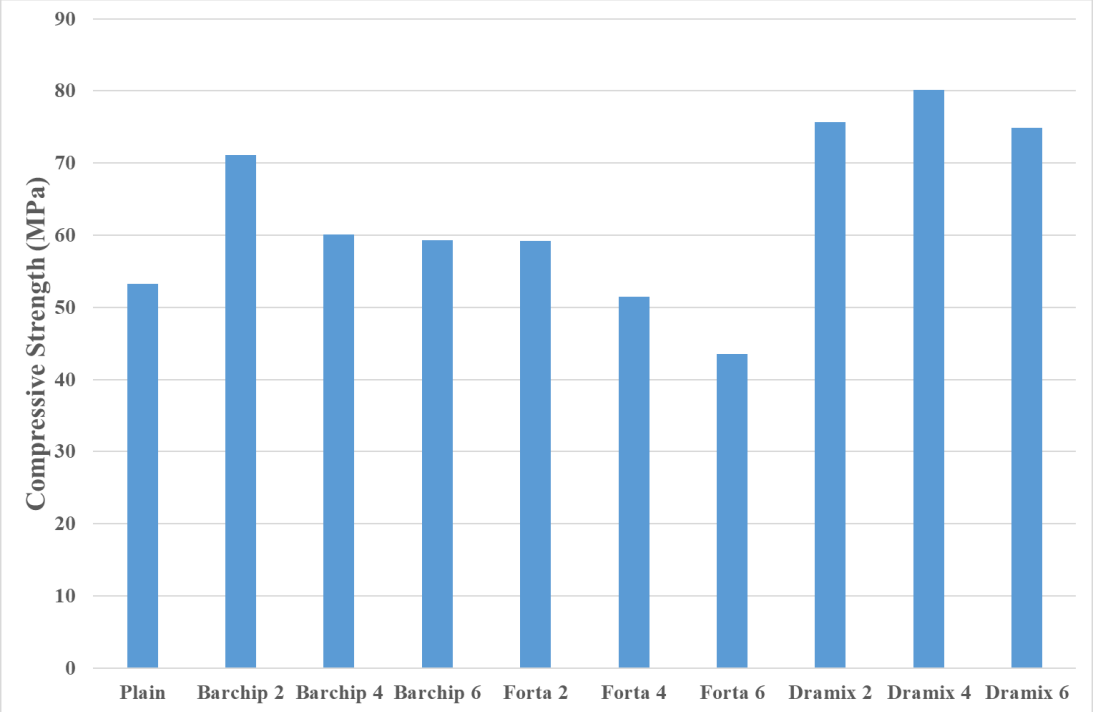

Figure 4.1. Bar Chart of Compression Test Results (Load-Controlled)

By using f_c value of the plain control specimen, f_t can be calculated as 3.91 MPa, according to the EuroCode.

Table 4.2. *Compressive Strength and Energy Absorption Values (Displacement-Controlled)*

Fiber Type	Fiber Content (%)	Compressive Strength (MPa)	Energy Absorption (Joule), at			
			Ultimate Load	0.05 Strain	0.10 Strain	0.15 Strain
Barchip	2	50.8	184.0	3158.5	4606.1	6050.7
	4	55.6	164.4	5412.4	8181.8	10172.2
	6	59.3	171.9	6992.9	10949.5	13660.6
Forta	2	58.7	151.7	3696.8	4908.8	5750.7
	4	52.8	153.8	5224.2	7767.0	9762.8
	6	51.5	139.4	4807.0	7195.5	8969.8
Dramix	2%	90.3	333.4	7381.2	11584.4	15921.4
	4%	95.9	363.9	8700.1	16460.6	24828.2
	6%	95.0	484.7	12335.5	22795.1	33823.7

* The color bar is applied for each column separately. Red for low and green for high.

4.2. Beam Bending Test

The average stress-displacement curves for each fiber type are presented in Figure 4.2 to Figure 4.4. Moreover, the energy-displacement curves for each fiber volume are presented in Figure 4.5 to Figure 4.7. In addition, the average flexural strength values and toughness values at different deflections are presented in **Hata! Başvuru kaynağı bulunamadı.**. Test results of all the specimens are given at Appendix A.

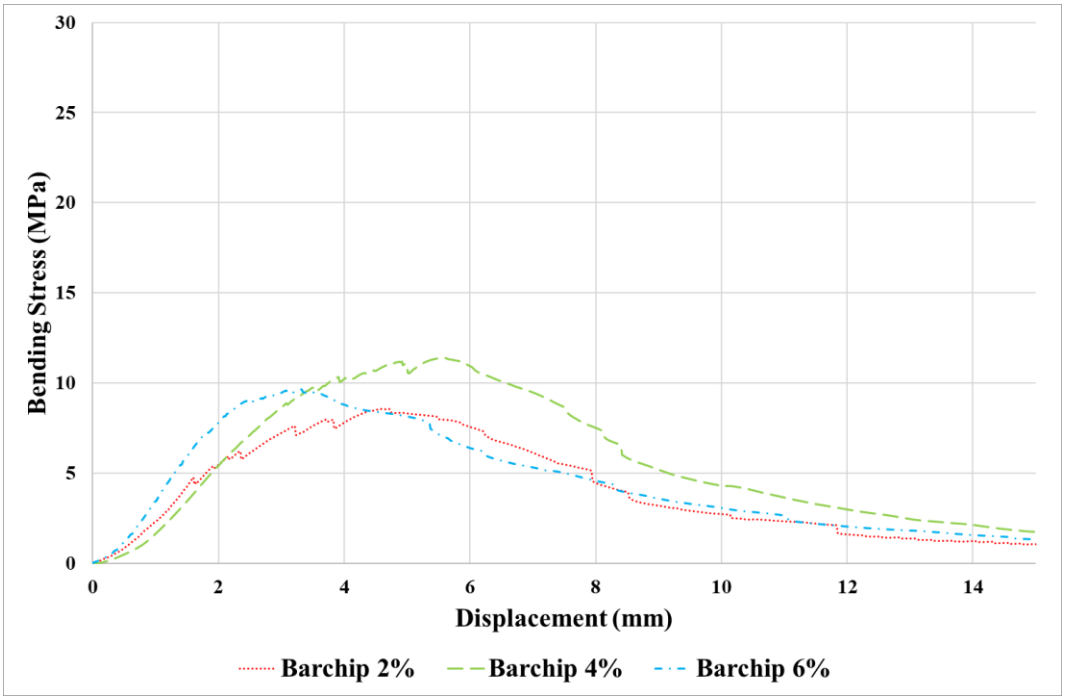

Figure 4.2. Bending Stress-Displacement Curves of Barchip Mixtures

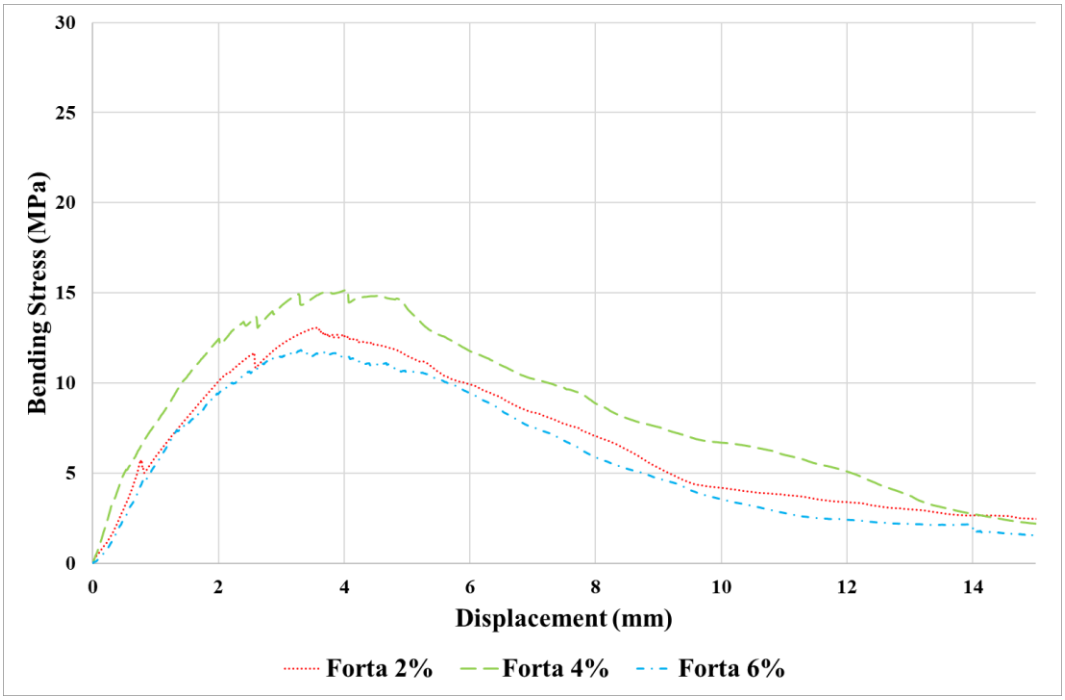

Figure 4.3. Bending Stress-Displacement Curves of Forta Mixtures

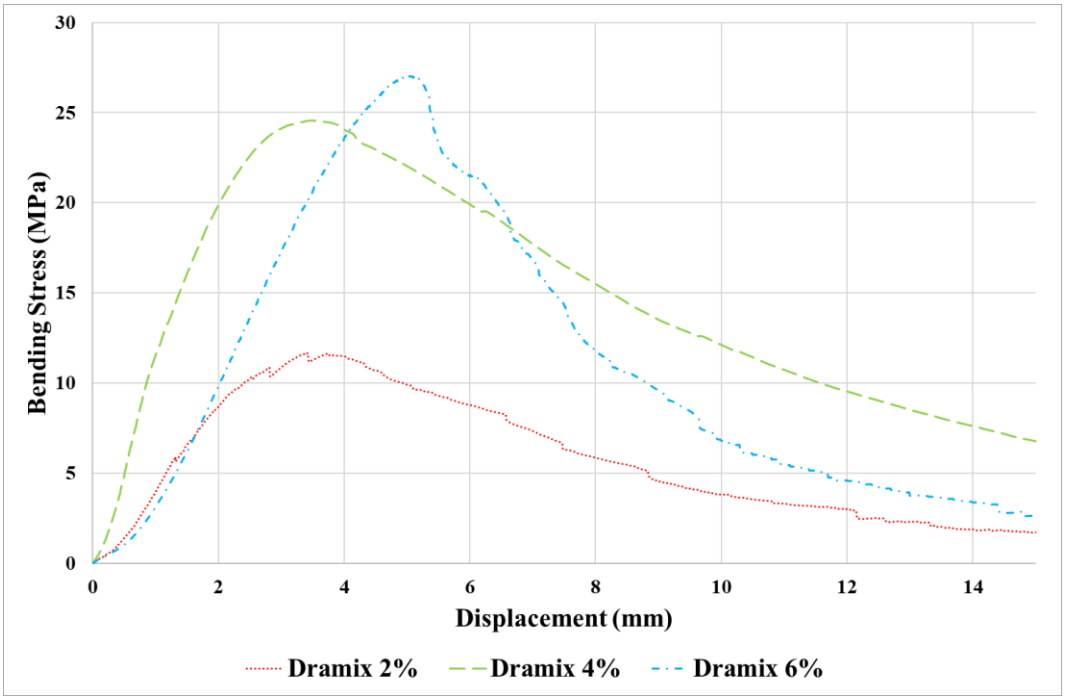

Figure 4.4. Bending Stress-Displacement Curves of Dramix Mixtures

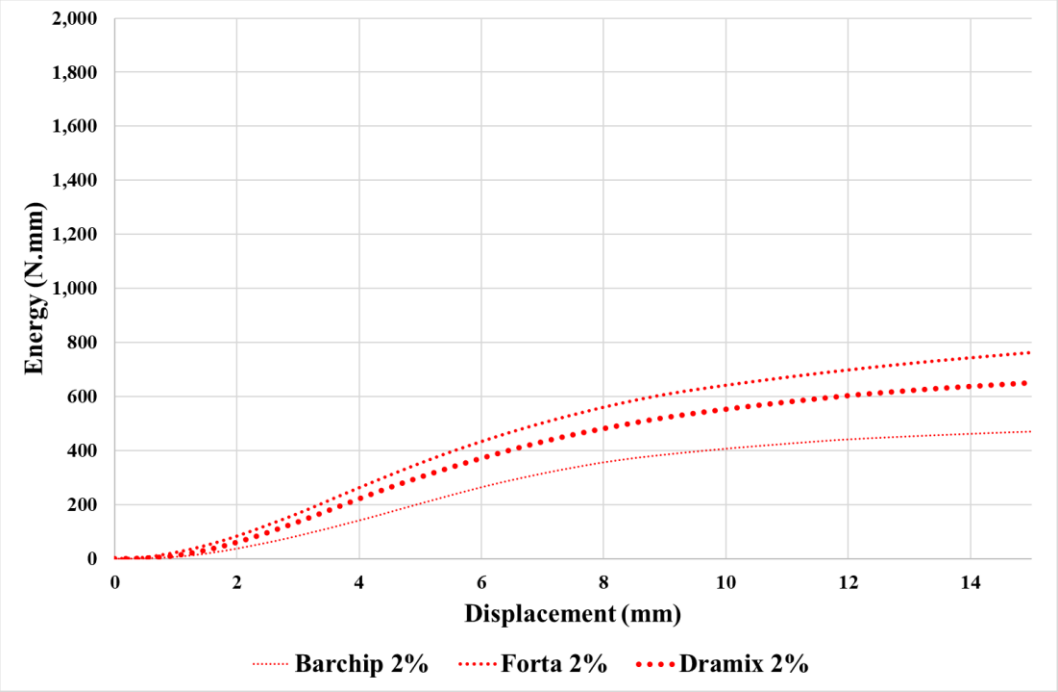

Figure 4.5. Energy-Displacement Curves of 2% Fiber Volume

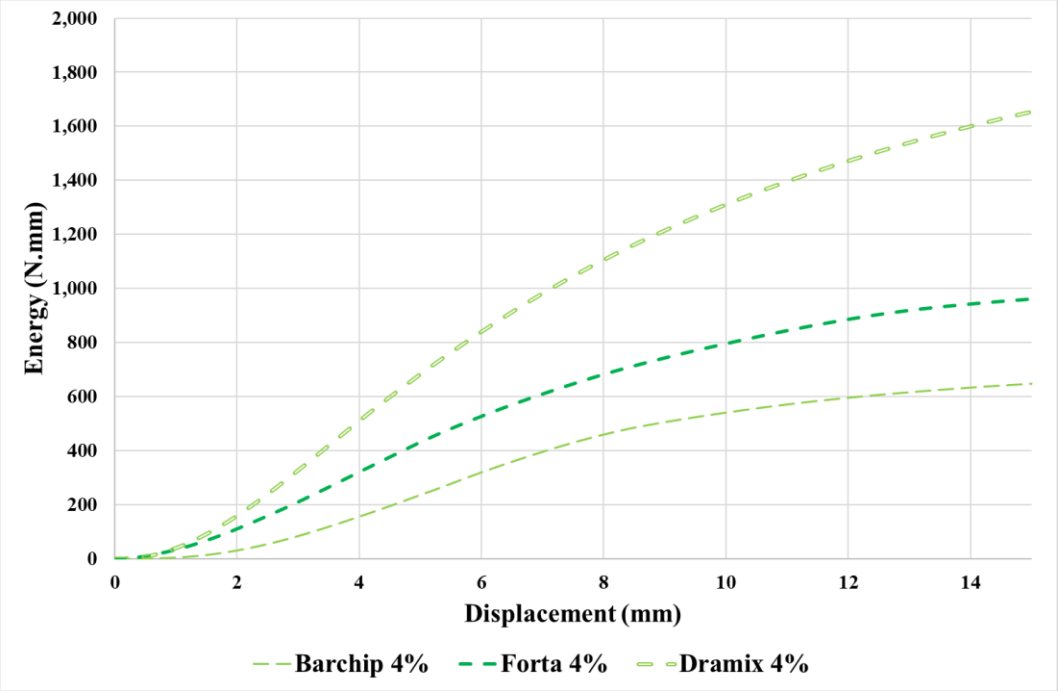

Figure 4.6. Energy-Displacement Curves of 4% Fiber Volume

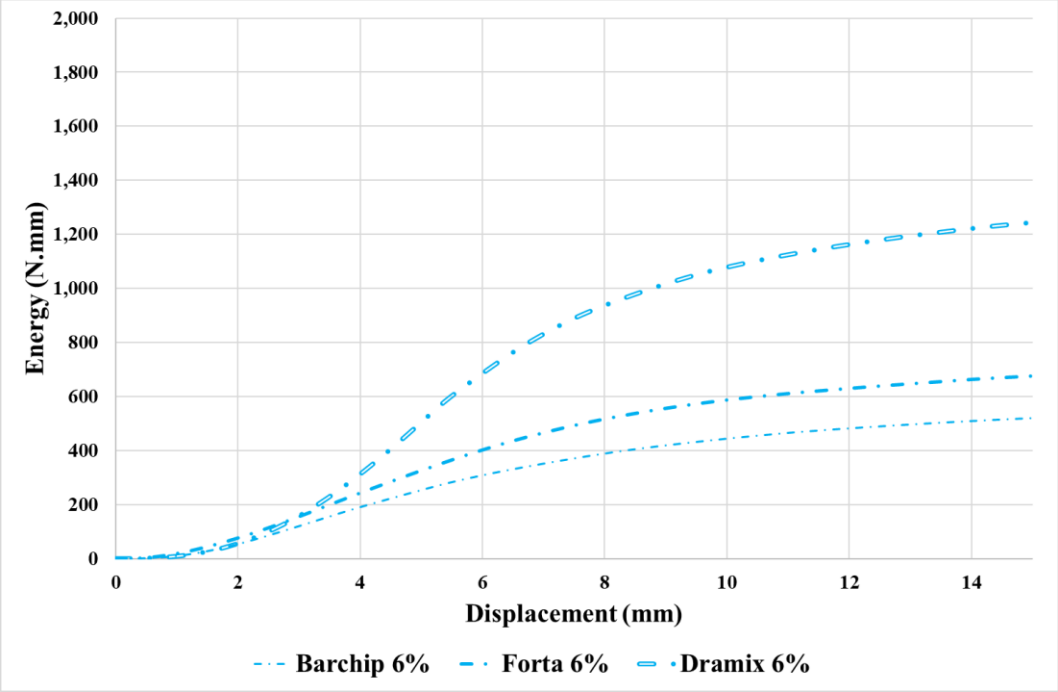

Figure 4.7. Energy-Displacement Curves of 6% Fiber Volume

Table 4.3. *Flexural Strength and Energy Absorption Values*

Fiber Type	Fiber Content (%)	Flexural Strength (MPa)	Energy Absorption (Joule), at				
			Ultimate Load	5 mm	10 mm	15 mm	20 mm
Barchip	2	8.6	177.7	204.3	407.2	470.6	497.5
	4	11.4	283.4	236	540.6	647.5	693.6
	6	9.7	142.2	254.1	444.3	520.3	558.5
Forta	2	13.1	223	353.8	641.9	762.9	836.7
	4	15.2	326.4	431.1	795.8	960.8	1021.3
	6	11.8	183.1	326.1	587.3	676	717.9
Dramix	2	11.7	172.1	302	553.2	651.1	700.7
	4	24.6	414.7	682.4	1310.4	1653.8	1854.6
	6	27.1	511.3	505.2	1078.8	1244	1328.5

* The color bar is applied for each column separately. Red for low and green for high.

Based on the test results, it can be said that for each fiber, the 4% dosage provides the best performance. For steel fibers of 6% dosage, the first specimen exceeded the capacity of the test machine, and the test was ended. However, when the second specimen reached the maximum capacity of the test device, the maximum load was held on the specimen until the applied load started to decrease. The maximum load for that specimen was derived based on a curve fitting the two sides of the peak. As for the third specimen, the ultimate load remained within the capacity of the machine. The reason why the 4% mixtures gave the best results, is the decrease in workability when the fiber amount was increased to 6%. This means that mortar used to bind the fibers became less effective for that amount of fibers. A change in the ingredients of the cementitious mortar might help to make the larger possible amount of fibers act under loading.

By using calculated f_t, σ of plain control specimen can be evaluated as 5.67 MPa, according to the EuroCode. Obtained flexural strength values of specimens and calculated strength values of plain control specimen are compared at Table 4.4.

Table 4.4. *Comparison of Flexural Strength*

Fiber Type	Fiber Content (%)	Flexural Strength (MPa)	Increase (%)
Plain Control	0	5.7	-
Barchip	2	8.6	51.68
	4	11.4	101.06
	6	9.7	71.08
Forta	2	13.1	131.04
	4	15.2	168.08
	6	11.8	108.11
Dramix	2	11.7	106.35
	4	24.6	333.86
	6	27.1	377.95

4.3. Splitting Tensile Strength Test

The average splitting tensile strength-COD curves for each fiber type are presented in Figure 4.8 to Figure 4.10. Moreover, the energy-displacement curves for each fiber volume are presented in Figure 4.11 to Figure 4.13. In addition, the average flexural strength values and toughness values at different deflections are presented in Table 4.5. Test results of all the specimens are given at Appendix B.

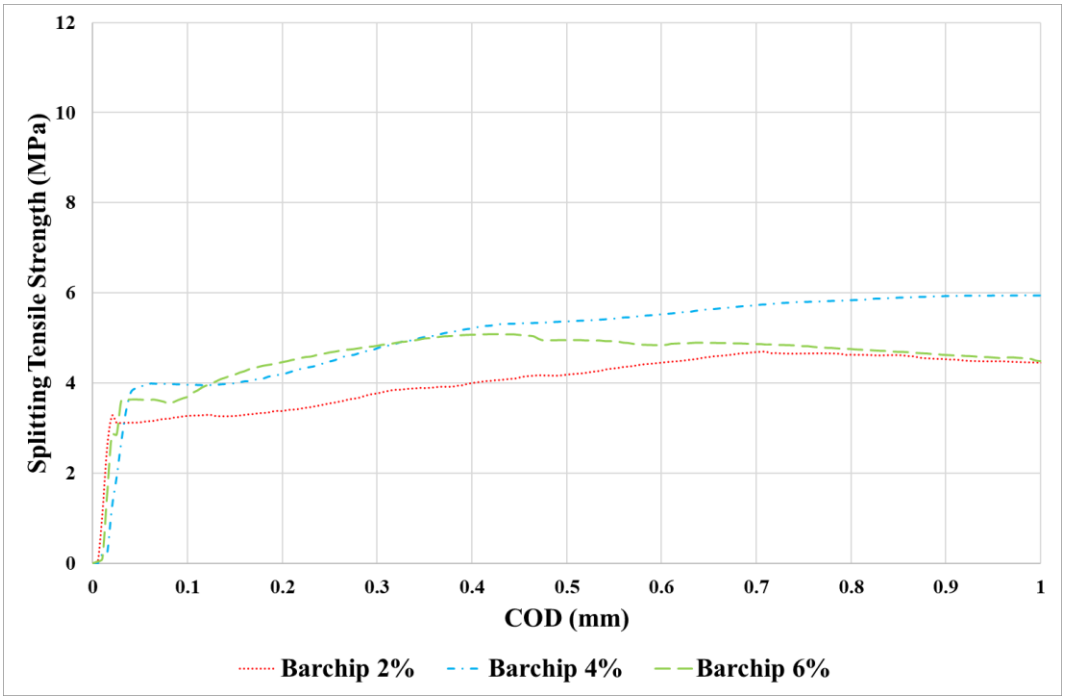

Figure 4.8. Splitting Tensile Strength Test Curves of Barchip Mixtures

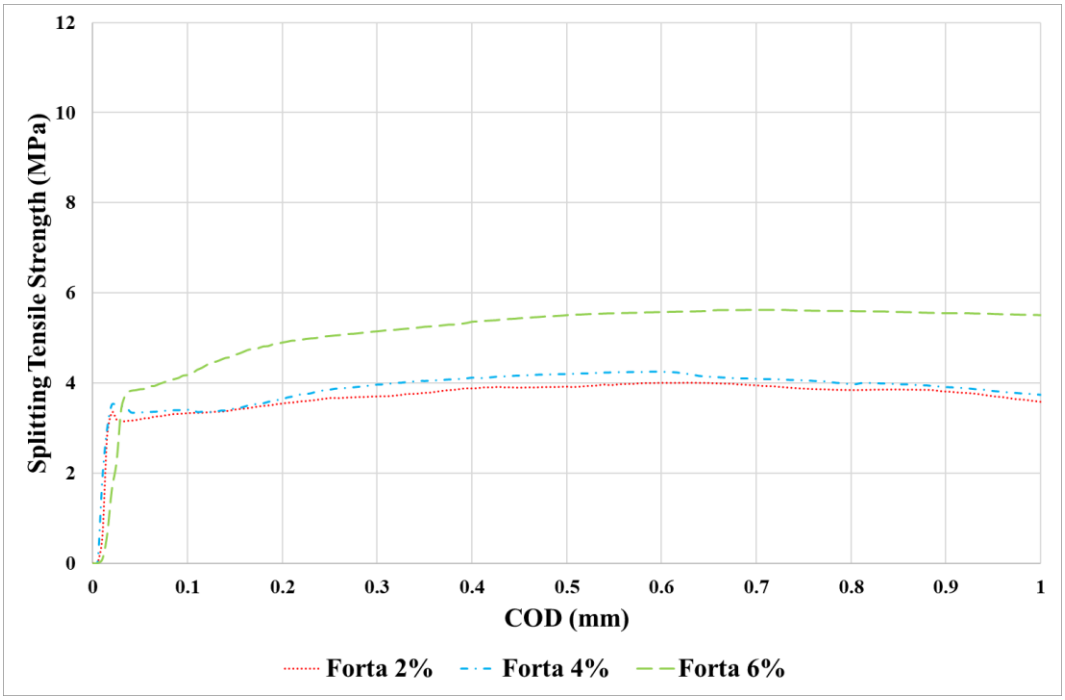

Figure 4.9. Splitting Tensile Strength Test Curves of Forta Mixtures

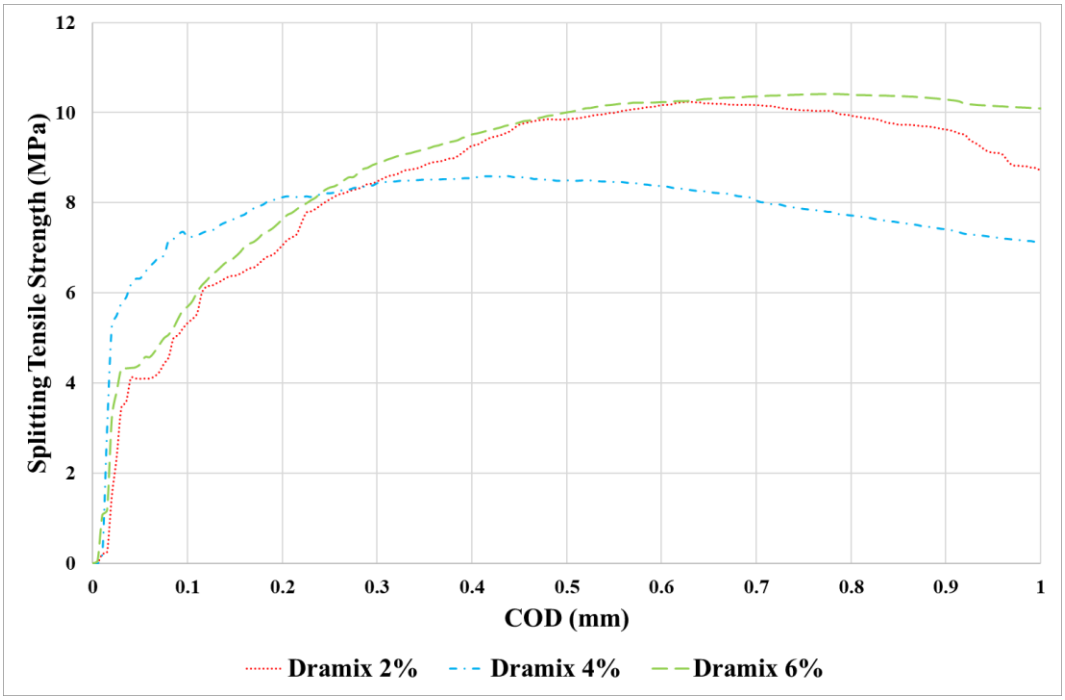

Figure 4.10. Splitting Tensile Strength Test Curves of Dramix Mixtures

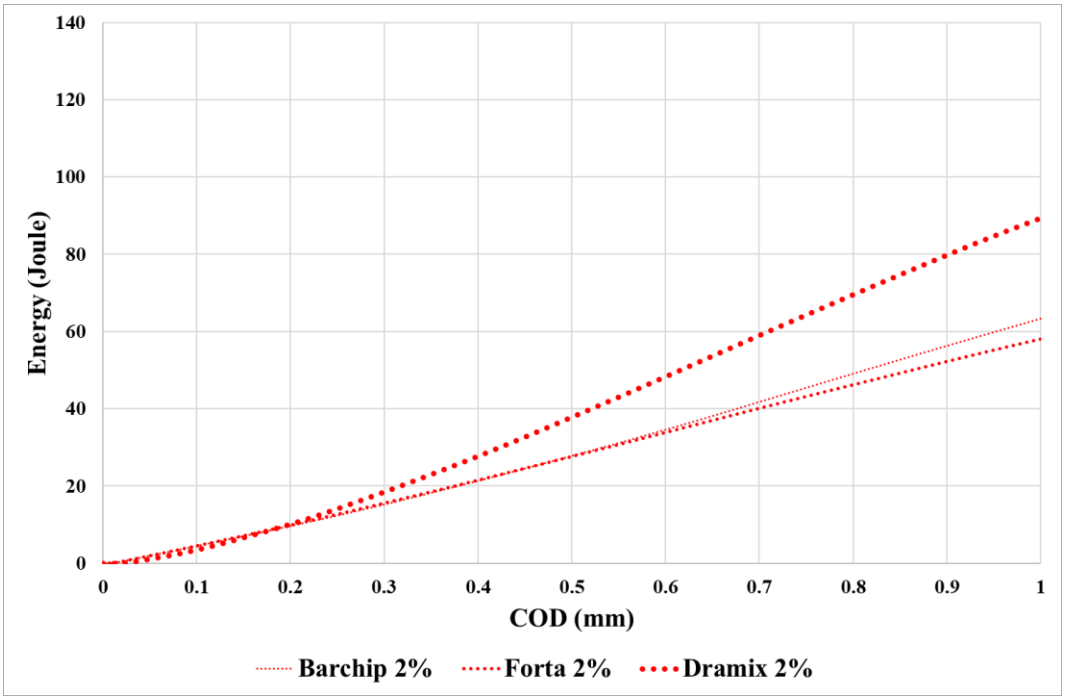

Figure 4.11. (Load×COD)-COD Curves of 2% Fiber Volume

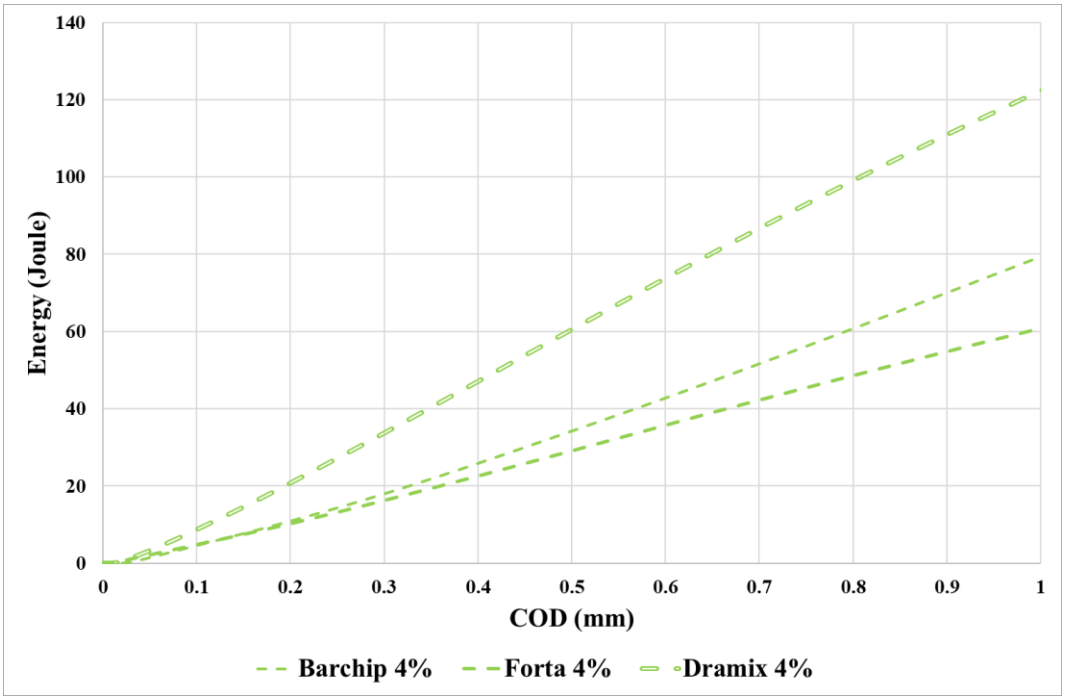

Figure 4.12. (Load×COD)-COD Curves of 4% Fiber Volume

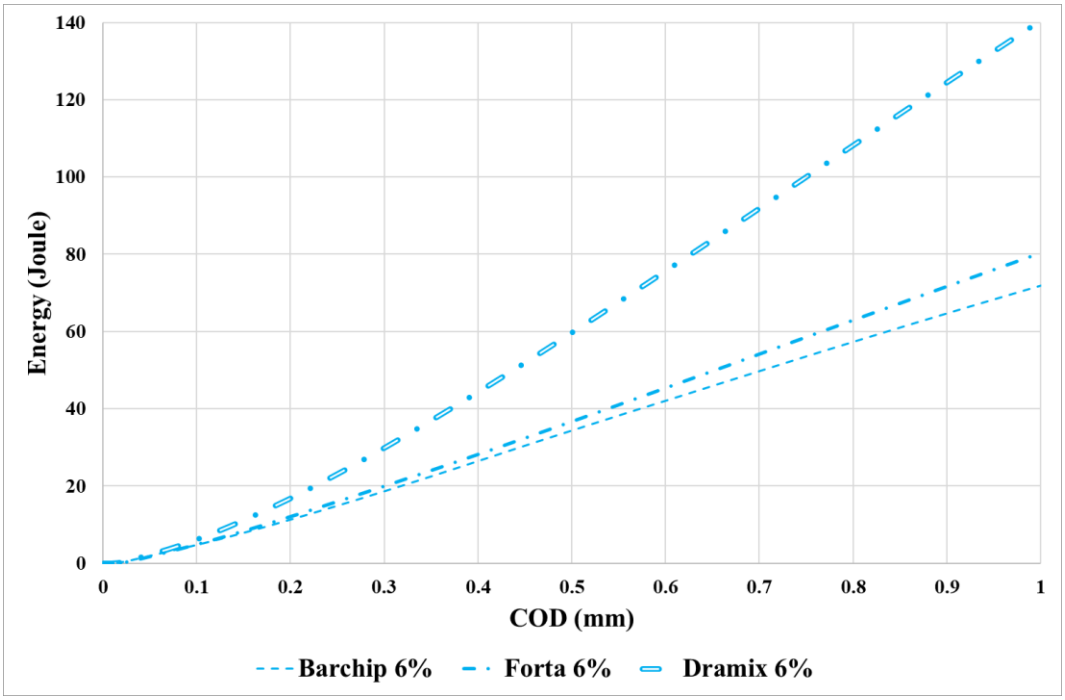

Figure 4.13. (Load×COD)-COD Curves of 6% Fiber Volume

Table 4.5. *Average Splitting Tensile Strength and Energy Absorption Values*

Fiber Type	Fiber Content (%)	Splitting Tensile Strength (MPa)	Load × COD (N.mm), at				
			Ultimate Load	0.2 mm	0.5 mm	0.7 mm	1 mm
Barchip	2	4.7	42.1	9.6	27.8	41.8	63.4
	4	5.9	77.9	11	34.2	51.6	79.3
	6	5.1	28.4	11.2	34.3	49.7	71.8
Forta	2	4	35.4	9.8	27.6	40.1	58.1
	4	4.2	35.4	10.2	29.1	42.3	60.8
	6	5.6	56.4	12	36.7	54.2	80.4
Dramix	2%	10.2	51.5	10.2	37.8	59	89.3
	4%	8.6	51.7	20.7	60.4	86.7	122.3
	6%	10.4	104.9	16.9	59.7	91.8	140.4

* The color bar is applied for each column separately. Red for low and green for high.

The splitting tensile strength tests also show that the increase in fiber amount lead to an increase in the tensile strength of FRC. Moreover, while the performances of the

two synthetic fibers were close to each other, steel fiber mixtures demonstrated a huge increase in general and for the same fiber volume as well. However, the most important outcome to point out of this test, is that for FRC mixtures, especially the ones containing a large amount of fibers, the splitting tensile test should be performed under displacement-controlled mode. When this test is done through the traditional load control mode, the test is usually ended at the first crack. However, it is clearly seen from the above figures, that the fibers start to act after that crack, and the ultimate splitting tensile keep increases after that point.

By using calculated f_t, $f_{t,sp}$ of reference specimen can be evaluated as 3.52 MPa, according to the EuroCode. The comparison of acquired splitting tensile strength test data with the calculated value is presented at Table 4.6.

Table 4.6. *Comparison of Splitting Tensile Strength*

Fiber Type	Fiber Content (%)	Splitting Tensile Strength (MPa)	Increase (%)
Plain Control	0	3.52	-
Barchip	2	4.7	33.52
	4	5.9	67.61
	6	5.1	44.89
Forta	2	4.0	13.64
	4	4.2	19.32
	6	5.6	59.09
Dramix	2	10.2	189.77
	4	8.6	144.32
	6	10.4	195.45

4.4. Comparison of Flexural and Splitting Tensile Strengths

According to EuroCode, flexural and splitting tensile strength values are correlated with each other and interchangeable by means of compressive strength for plain concrete. With the data of the tests, strength and energy graphs are sketched in Figure 4.14 and Figure 4.15, respectively.

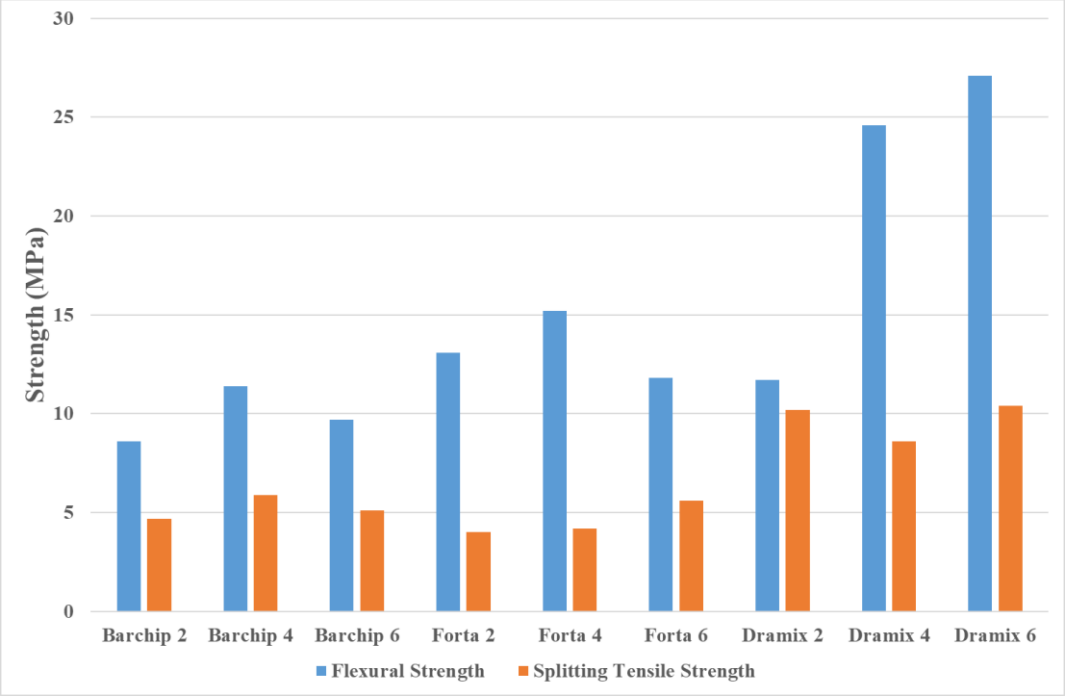

Figure 4.14. Graph of Flexural and Splitting Tensile Strengths

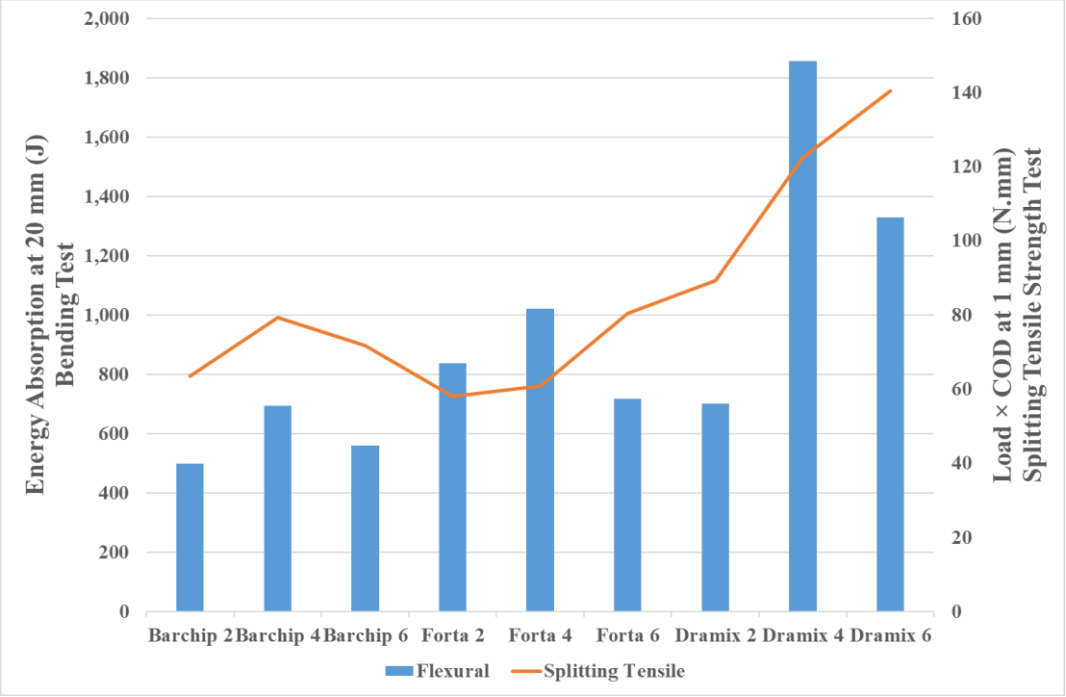

Figure 4.15. Graph of Energy Absorption in Bending Test and Load×COD in Splitting Tensile Strength Test

To see the correlation in between, Figure 4.16 and Figure 4.17 are prepared. As can be seen, the rules stated in EuroCode are not applicable to high-dosage FRC produced in this study.

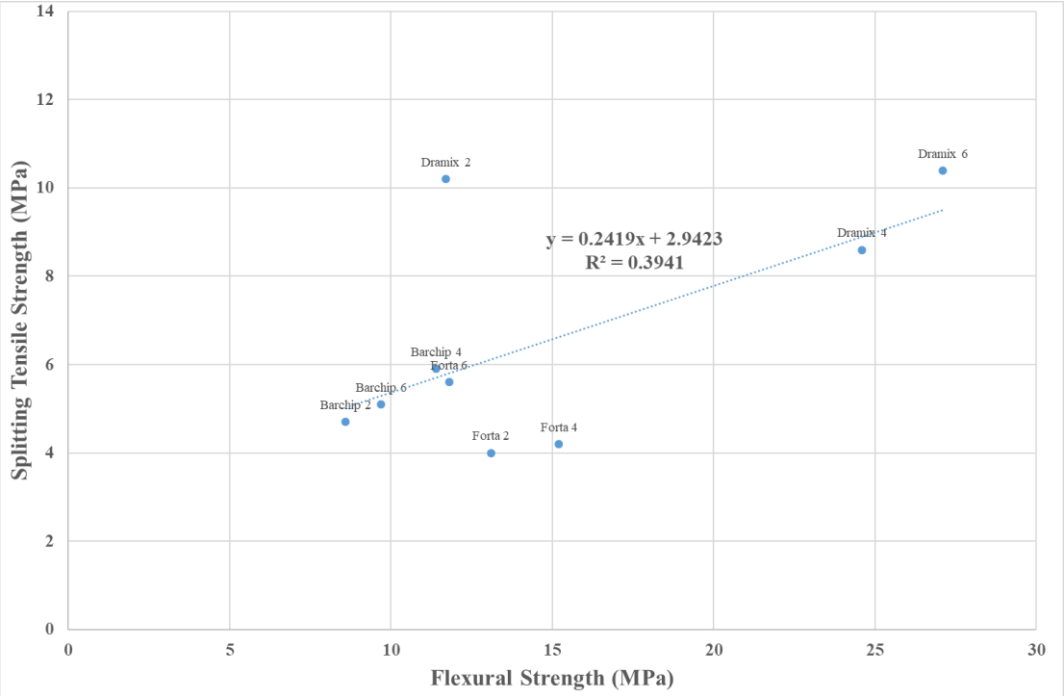

Figure 4.16. Correlation Graph of Strength Values

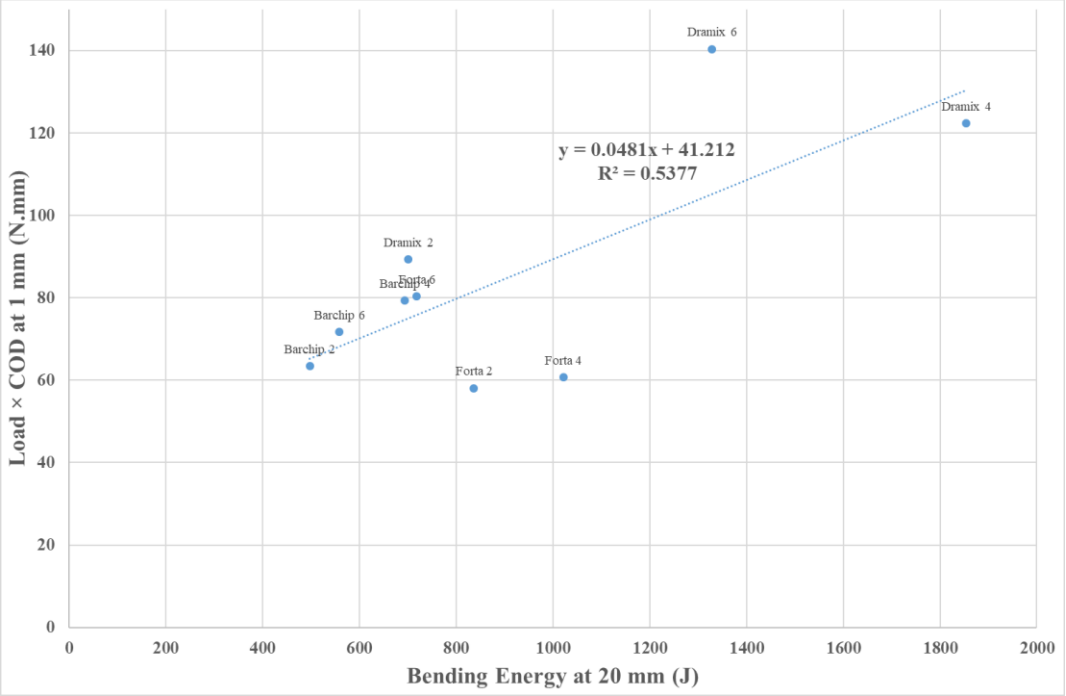

Figure 4.17. Correlation Graph of Energy Absorption in Bending Test and Load×COD in Splitting Tensile Strength Test

4.5. Equivalent Steel Rebar Calculations

With the data collected in beam bending tests, the moment capacity of the specimens can be determined. The total cross-sectional area of tension reinforcement can be calculated through the following formula:

$$A_s = \frac{M}{j d_s f_{yd}}$$

where;

A_s is the total cross-sectional area of rebars in mm^2,

M is moment at ultimate loading case in N.mm,

j is balanced moment arm factor, taken as 0.782 for this test set up and specimens,

d_s is depth of rebar in mm, taken as 130 mm with 2 cm of clear cover,

f_{yd} is tensile yield strength of rebars in MPa, taken as 420 MPa for S420 steel.

Accordingly, the calculated rebar cross-sectional areas and the equivalent number of Ø14 bars of S420 steel for 150×150 mm^2 surface area under flexure are listed at Table 4.7.

Table 4.7. *Equivalent Steel Rebar Comparison*

Fiber Type	Fiber Content (%)	Max Load (kN)	Moment (kN.m)	Steel Area (mm^2)	# of Ø14 Bars (S420)
Barchip	2	64.32	9.65	225.98	2
	4	85.55	12.83	300.54	2
	6	72.38	10.86	254.29	2
Forta	2	98.08	14.71	344.57	3
	4	113.99	17.10	400.47	3
	6	88.74	13.31	311.75	3
Dramix	2	87.47	13.12	307.29	2
	4	184.25	27.63	647.28	5
	6	203.00	30.45	713.16	5

CHAPTER 5

CONCLUSION AND RECOMMENDATIONS

5.1. Conclusion

In this work, three different fibers (two synthetic and one steel) were added to concrete in high amounts (2%, 4%, and 6% of volume). Knowing that the use of fibers can highly improve the mechanical properties of concrete, yet, with more fibers the workability can greatly decrease, the aim of this study was to produce castable high fiber dosage concrete mixtures. Different from the other attempts or researches that use a high-volume fraction of fibers, in this work fine aggregate (0-4 mm) was used in the concrete mixtures in order to reduce the volume instability problems and the cost of concrete. Based on the test results, the following conclusions can be drawn.

- With fiber ratios of 2% and 4% of volume, castable self-consolidating concrete mixtures were successfully produced. When fiber volume was increased to 6%, a mechanical vibrator needed to fill the molds properly.

- As expected, the increase in fiber volume lead to improvement in the mechanical performance of FRC. However, for most of the mixtures, the differences between the 4% and the 6% performances were not that significant, and in some cases the 4% mixtures demonstrated better performance. This can be attributed to two main reasons. The first one is the lack of proper compaction in 6% mixtures, and the second one is insufficiency of the cementitious mortar to make the whole amount of fiber act for that dosage.

- The effects of fiber type and properties were clearly seen through the test results. When the ultimate strengths and the energy values are examined, mixtures with steel fibers showed the best performance in almost all the tests. As for the synthetic fibers, there was no significant pattern for the difference between single or bundle type fibers. Comparing with the values evaluated from compression of reference specimen, using fibers increased tensile capacity of the batch tremendously; 52% to 378% increment in flexural, 14% to 195% increase in splitting tensile strength were recorded.

- Even if it might not be feasible economically, by using this type of FRC mixtures, rebar-free concrete structural elements can be prepared and examined. For some cases where the construction time is the governing concern, high-dosage FRC members can be cast instead of conventional reinforced concrete to save the time of rebar preparation and installation, especially in the production of precast concrete elements.

- The post-cracking performance of the tested FRC mixtures showed that applying a displacement control test is highly important, especially for splitting tensile strength test, in order to obtain the true behavior of such mixtures.

5.2. Recommendations

Based on the test results and the conclusions made above, the following recommendations are suggested for future studies.

- The mixture design can be optimized and improved to get better results of higher fiber dosages with the help of consistency regulating chemicals.

- The traditional test method used for self-consolidating concrete are not suitable for such mixtures. While the steel bars found in the J-ring and the L Box prevent the high amount of fibers from passing through, the waiting period and the shape of the slump cone and U box test can lead to an accumulation of fibers at the middle while the grout flows separately. For that, a modified test can be developed, or the mixture design can be improved to adopt those tests to monitor the fresh properties.

- The durability and volume stability of high-dosage FRC can be examined.

- Similar FRC mixtures can be prepared with hybrid fibers to determine the effects of such combinations on the fresh and hardened properties of FRC.

The performance high-dosage FRC under impact, explosion, and ballistic cases can be examined.

REFERENCES

Aarthi, K., & Arunachalam, K. (2018). Durability studies on fibre reinforced self compacting concrete with sustainable wastes. *Journal of Cleaner Production*, *174*, 247–255. https://doi.org/10.1016/J.JCLEPRO.2017.10.270

Abbass, W., Khan, M. I., & Mourad, S. (2018). Evaluation of mechanical properties of steel fiber reinforced concrete with different strengths of concrete. *Construction and Building Materials*, *168*, 556–569. https://doi.org/10.1016/J.CONBUILDMAT.2018.02.164

Abrishambaf, A., Barros, J. A. O., & Cunha, V. M. C. F. (2015). Tensile stress–crack width law for steel fibre reinforced self-compacting concrete obtained from indirect (splitting) tensile tests. *Cement and Concrete Composites*, *57*, 153–165. https://doi.org/10.1016/J.CEMCONCOMP.2014.12.010

Afroughsabet, V., & Ozbakkaloglu, T. (2015). Mechanical and durability properties of high-strength concrete containing steel and polypropylene fibers. *Construction and Building Materials*. https://doi.org/10.1016/j.conbuildmat.2015.06.051

Afroz, M., Patnaikuni, I., & Venkatesan, S. (2017). Chemical durability and performance of modified basalt fiber in concrete medium. *Construction and Building Materials*, *154*, 191–203. https://doi.org/10.1016/J.CONBUILDMAT.2017.07.153

Akkaya, Y., Shah, S. P., & Ankenman, B. (2001). Effect of Fiber Dispersion on Multiple Cracking of Cement Composites. *Journal of Engineering Mechanics*, *127(4)*, 311–316. Retrieved from https://doi.org/10.1061/(ASCE)0733-9399(2001)127:4(311)

Alhussainy, F., Hasan, H. A., Rogic, S., Neaz Sheikh, M., & Hadi, M. N. S. (2016). Direct tensile testing of Self-Compacting Concrete. *Construction and Building Materials*, *112*, 903–906. https://doi.org/10.1016/J.CONBUILDMAT.2016.02.215

Alnahhal, W., & Aljidda, O. (2018). Flexural behavior of basalt fiber reinforced concrete beams with recycled concrete coarse aggregates. *Construction and Building Materials*, *169*, 165–178. https://doi.org/10.1016/J.CONBUILDMAT.2018.02.135

American Concrete Institute. (2002). Report on Fiber Reinforced Concrete. *Report on Reinforced Concrete (Reapproved). ACI Committee 544. Detroit, 96*(Reapproved 2009), 1–66. Retrieved from http://indiafiber.com/Files/ACI

report.pdf

Bae, B.-I., Chung, J.-H., Choi, H.-K., Jung, H.-S., & Choi, C.-S. (2018). Experimental study on the cyclic behavior of steel fiber reinforced high strength concrete columns and evaluation of shear strength. *Engineering Structures*, *157*, 250–267. https://doi.org/10.1016/J.ENGSTRUCT.2017.11.072

Balaguru, P. N., & Shah, S. P. (1992). *Fiber-reinforced cement composites*.

Bangi, M. R., & Horiguchi, T. (2012). Effect of fibre type and geometry on maximum pore pressures in fibre-reinforced high strength concrete at elevated temperatures. *Cement and Concrete Research*, *42*(2), 459–466. https://doi.org/10.1016/J.CEMCONRES.2011.11.014

Banthia, N., & Dubey, A. (1999). Measurement of flexural toughness of fiber-reinforced concrete using a novel technique—part 1: assessment and calibration. *Materials Journal*, *96*(6), 651–656.

Bentur, A., & Mindess, S. (2007). *Fibre Reinforced Cementitious Composites*. *Modern Concrete Technology Series* (2nd Ed.). London and New York: Taylor and Francis Group.

Betterman, L. R., Ouyang, C., & Shah, S. P. (1995). Fiber-matrix interaction in microfiber-reinforced mortar. *Advanced Cement Based Materials*, *2*(2), 53–61. https://doi.org/10.1016/1065-7355(95)90025-X

Bilba, K., Arsene, M.-A., & Ouensanga, A. (2003). Sugar cane bagasse fibre reinforced cement composites. Part I. Influence of the botanical components of bagasse on the setting of bagasse/cement composite. *Cement and Concrete Composites*, *25*(1), 91–96. https://doi.org/10.1016/S0958-9465(02)00003-3

Bothma, J. (2013). *Literature Review on Macro Synthetic Fibres in Concrete*.

Brandt, A. M. (2008). Fibre reinforced cement-based (FRC) composites after over 40 years of development in building and civil engineering. *Composite Structures*. https://doi.org/10.1016/j.compstruct.2008.03.006

Carmona, S., & Aguado, A. (2012). New model for the indirect determination of the tensile stress-strain curve of concrete by means of the Brazilian test. *Materials and Structures*, *45*(10), 1473–1485. https://doi.org/10.1617/s11527-012-9851-0

Chen, M., Gao, P., Geng, F., Zhang, L., & Liu, H. (2017). Mechanical and smart properties of carbon fiber and graphite conductive concrete for internal damage monitoring of structure. *Construction and Building Materials*, *142*, 320–327. https://doi.org/10.1016/J.CONBUILDMAT.2017.03.048

Chu, S. H., Li, L. G., & Kwan, A. K. H. (2018). Fibre factors governing the fresh and hardened properties of steel FRC. *Construction and Building Materials*, *186*, 1228–1238. https://doi.org/10.1016/J.CONBUILDMAT.2018.08.047

Curosu, I., Mechtcherine, V., & Millon, O. (2016). Effect of fiber properties and matrix composition on the tensile behavior of strain-hardening cement-based composites (SHCCs) subject to impact loading. *Cement and Concrete Research*, *82*, 23–35. https://doi.org/10.1016/J.CEMCONRES.2015.12.008

Destree, X. (2004). Structural application of steel fibres as only reinforcing in free suspended elevated slabs: conditions–Design examples. In *Sixth RILEM Symposium on fibre reinforced concrete Varenna/Italy* (Vol. 2, pp. 1073–1082).

Ding, Y., & Kusterle, W. (1999). Comparative study of steel fibre-reinforced concrete and steel mesh-reinforced concrete at early ages in panel tests. *Cement and Concrete Research*, *29*(11), 1827–1834. https://doi.org/10.1016/S0008-8846(99)00177-5

Erdoğan, S. T., & Erdoğan, T. Y. (2014). *Basic Materials of Construction*. Ankara: METU Press.

ETH Zurich. (2016). Mechanics and Failure of Fibre Reinforced Composites (FRC). Retrieved June 4, 2019, from https://www.ethz.ch/content/dam/ethz/special-interest/baug/ifb/ifb-dam/homepage-IfB/Education/msc_courses/msc-materials-IV/documents/W4_Fibers_2016.pdf

Grünewald, S. (2012). Fibre reinforcement and the rheology of concrete. *Understanding the Rheology of Concrete*, 229–256. https://doi.org/10.1533/9780857095282.2.229

Hetemoğlu, Y. O. (2018). *Effect of Test Methods on The Performance of Fiber Reinforced Concrete with Different Dosages and Matrices*. Middle East Technical University.

Jen, G., Trono, W., & Ostertag, C. P. (2016). Self-consolidating hybrid fiber reinforced concrete: Development, properties and composite behavior. *Construction and Building Materials*. https://doi.org/10.1016/j.conbuildmat.2015.12.062

Junker, F., Holschemacher, K., Müller, T., & Kieslich, H. (2017). Replacement of minimum steel bar reinforcement with steel fibres in structural concrete members. *IOP Conference Series: Materials Science and Engineering*, *246*, 12003. https://doi.org/10.1088/1757-899x/246/1/012003

Kim, M.-J., Yoo, D.-Y., Kim, S., Shin, M., & Banthia, N. (2018). Effects of fiber

geometry and cryogenic condition on mechanical properties of ultra-high-performance fiber-reinforced concrete. *Cement and Concrete Research*, *107*, 30–40. https://doi.org/10.1016/J.CEMCONRES.2018.02.003

Lee, J.-H. (2017). Influence of concrete strength combined with fiber content in the residual flexural strengths of fiber reinforced concrete. *Composite Structures*, *168*, 216–225. https://doi.org/10.1016/J.COMPSTRUCT.2017.01.052

Lee, J.-Y., Shin, H.-O., Yoo, D.-Y., & Yoon, Y.-S. (2018). Structural response of steel-fiber-reinforced concrete beams under various loading rates. *Engineering Structures*, *156*, 271–283. https://doi.org/10.1016/J.ENGSTRUCT.2017.11.052

Li, V. C. (2002a). Advances in ECC research. *ACI Special Publications*, *206*, 373–400.

Li, V. C. (2002b). Large Volume, High-Performance Applications of Fibers in Civil Engineering. *Journal of Applied Polymer Science*, *83*, 660–686. https://doi.org/10.1002/app

Malhotra, V. M. (1980). *Progress in concrete technology*.

Mansur, M. A., & Aziz, M. A. (1982). A study of jute fibre reinforced cement composites. *International Journal of Cement Composites and Lightweight Concrete*, *4*(2), 75–82. https://doi.org/10.1016/0262-5075(82)90011-2

Mehta, K. P., & Monteiro, P. J. M. (2006). *Concrete Microstructure, Properties, and Materials* (Third). McGraw-Hill.

Molins, C., Aguado, A., & Saludes, S. (2009). Double Punch Test to control the energy dissipation in tension of FRC (Barcelona test). *Materials and Structures*, *42*(4), 415–425. https://doi.org/10.1617/s11527-008-9391-9

Mostafazadeh, M., & Abolmaali, A. (2016). Shear Behavior of Synthetic Fiber Reinforced Concrete. *Advances in Civil Engineering Materials*, *5*(1), 371–386. https://doi.org/10.1520/ACEM20160005

Naaman, A. E. (1998). New fiber technology (cement, ceramic, and polymeric composites). *Concrete International*, *20*(7), 57–62.

Neville, A. M. (1995). *Properties of concrete* (Vol. 4). longman London.

Onuaguluchi, O., & Banthia, N. (2016). Plant-based natural fibre reinforced cement composites: A review. *Cement and Concrete Composites*, *68*, 96–108. https://doi.org/10.1016/J.CEMCONCOMP.2016.02.014

Ortega-López, V., Fuente-Alonso, J. A., Santamaría, A., San-José, J. T., & Aragón,

Á. (2018). Durability studies on fiber-reinforced EAF slag concrete for pavements. *Construction and Building Materials*, *163*, 471–481. https://doi.org/10.1016/J.CONBUILDMAT.2017.12.121

Othman, H., Marzouk, H., & Sherif, M. (2019). Effects of variations in compressive strength and fibre content on dynamic properties of ultra-high performance fibre-reinforced concrete. *Construction and Building Materials*, *195*, 547–556. https://doi.org/10.1016/J.CONBUILDMAT.2018.11.093

Pająk, M., & Ponikiewski, T. (2013). Flexural behavior of self-compacting concrete reinforced with different types of steel fibers. *Construction and Building Materials*, *47*, 397–408. https://doi.org/10.1016/J.CONBUILDMAT.2013.05.072

Savastano, H., Agopyan, V., Nolasco, A. M., & Pimentel, L. (1999). Plant fibre reinforced cement components for roofing. *Construction and Building Materials*, *13*(8), 433–438. https://doi.org/10.1016/S0950-0618(99)00046-X

Shadravan, B., & Tehrani, F. (2017). A Review of Direct Shear Testing Configurations for Bond between Fiber-Reinforced Polymer Sheets on Concrete and Masonry Substrates. *Periodica Polytechnica Civil Engineering*, *61*(4 SE-Research Article). https://doi.org/https://doi.org/10.3311/PPci.9090

Shah, S. P., & Naaman, A. E. (1976). Mechanical Properties of Glass and Steel Fiber Reinforced Mortar. *ACI Journal Proceedings*, *73*(1). https://doi.org/10.14359/11055

Shin, K. J., Jang, K. H., Choi, Y. C., & Lee, S. C. (2015). Flexural behavior of HPFRCC members with inhomogeneous material properties. *Materials*, *8*(4), 1934–1950. https://doi.org/10.3390/ma8041934

Soltanzadeh, F., Barros, J. A. O., & Santos, R. F. C. (2015). High performance fiber reinforced concrete for the shear reinforcement: Experimental and numerical research. *Construction and Building Materials*, *77*, 94–109. https://doi.org/10.1016/J.CONBUILDMAT.2014.12.003

Soroushian, P., & Bayasi, Z. (1991). *Fiber-type effects on the performance of steel fiber reinforced concrete*. *ACI Materials Journal* (Vol. 88).

Soufeiani, L., Raman, S. N., Jumaat, M. Z. Bin, Alengaram, U. J., Ghadyani, G., & Mendis, P. (2016). Influences of the volume fraction and shape of steel fibers on fiber-reinforced concrete subjected to dynamic loading – A review. *Engineering Structures*, *124*, 405–417. https://doi.org/10.1016/J.ENGSTRUCT.2016.06.029

Steinmann, W.; Walter, S.; Beckers, M.; Seide, G.; Gries, T. (2013). Thermal Analysis

of Phase Transitions ans Crystallization in Polymeric Fibers. *Applications of Calorimetry in a Wide Context - Differential Scanning Calorimetry, Isothermal Titration Calorimetry and Microcalorimetry*, (tourism), 13. https://doi.org/http://dx.doi.org/10.5772/54063

Sudin, R., & Swamy, N. (2006). Bamboo and wood fibre cement composites for sustainable infrastructure regeneration. *Journal of Materials Science*, *41*(21), 6917–6924. https://doi.org/10.1007/s10853-006-0224-3

Tjiptobroto, P., & Hansen, W. (1991). Mechanism for tensile strain hardening in high performance cement-based fiber reinforced composites. *Cement and Concrete Composites*, *13*(4), 265–273. https://doi.org/10.1016/0958-9465(91)90032-D

Tokyay, M. (2016). *Cement and Concrete Mineral Admixtures*. CRC Press, Taylor&Francis Group.

Xu, Z., Hao, H., & Li, H. N. (2012). Dynamic tensile behaviour of fibre reinforced concrete with spiral fibres. *Materials & Design*, *42*, 72–88. https://doi.org/10.1016/J.MATDES.2012.05.047

Yoo, D.-Y., & Banthia, N. (2017). Mechanical and structural behaviors of ultra-high-performance fiber-reinforced concrete subjected to impact and blast. *Construction and Building Materials*, *149*, 416–431. https://doi.org/10.1016/J.CONBUILDMAT.2017.05.136

Yoo, D.-Y., Yoon, Y.-S., & Banthia, N. (2015). Flexural response of steel-fiber-reinforced concrete beams: Effects of strength, fiber content, and strain-rate. *Cement and Concrete Composites*, *64*, 84–92. https://doi.org/10.1016/J.CEMCONCOMP.2015.10.001

Yousefieh, N., Joshaghani, A., Hajibandeh, E., & Shekarchi, M. (2017). Influence of fibers on drying shrinkage in restrained concrete. *Construction and Building Materials*, *148*, 833–845. https://doi.org/10.1016/J.CONBUILDMAT.2017.05.093

Zhao, Q., Yu, J., Geng, G., Jiang, J., & Liu, X. (2016). Effect of fiber types on creep behavior of concrete. *Construction and Building Materials*, *105*, 416–422. https://doi.org/10.1016/J.CONBUILDMAT.2015.12.149

Zollo, R. F. (1984). Collated Fibrillated Polypropylene Fibers in FRC. *Special Publication*, *81*. https://doi.org/10.14359/6461

Zollo, R. F. (1997). Fiber-reinforced concrete: an overview after 30 years of development. *Cement and Concrete Composites*, *19*(2), 107–122. https://doi.org/10.1016/S0958-9465(96)00046-7

APPENDICES

A. Beam Bending Test Curves

Load-Deflection Curves

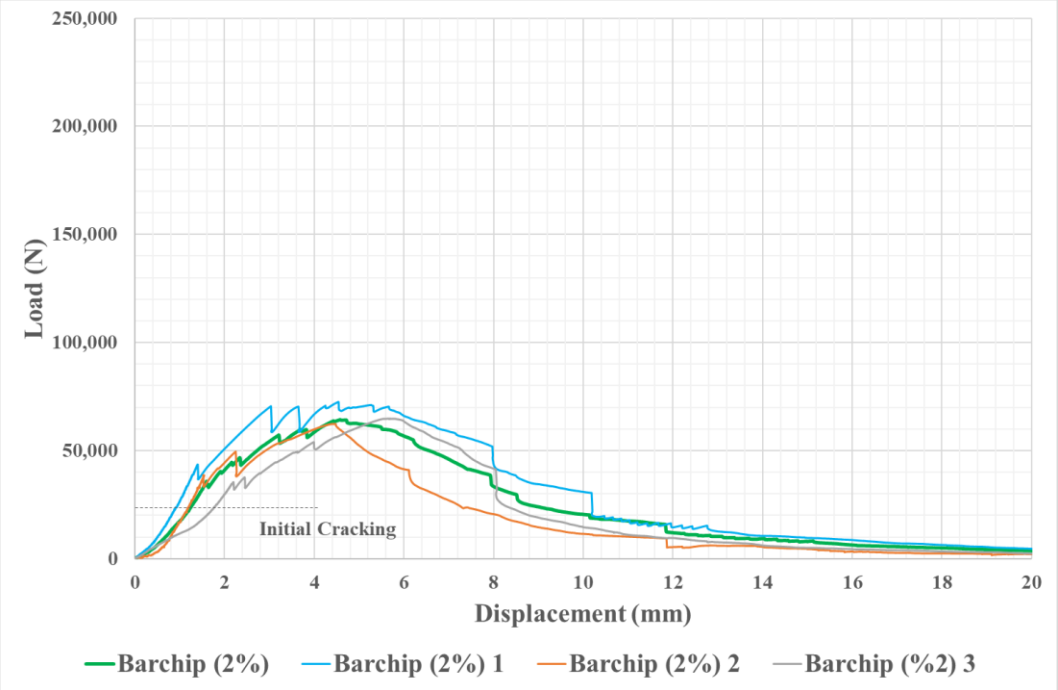

Figure A.1. Load-Deflection Curves of FRC with Barchip Fibers 2%

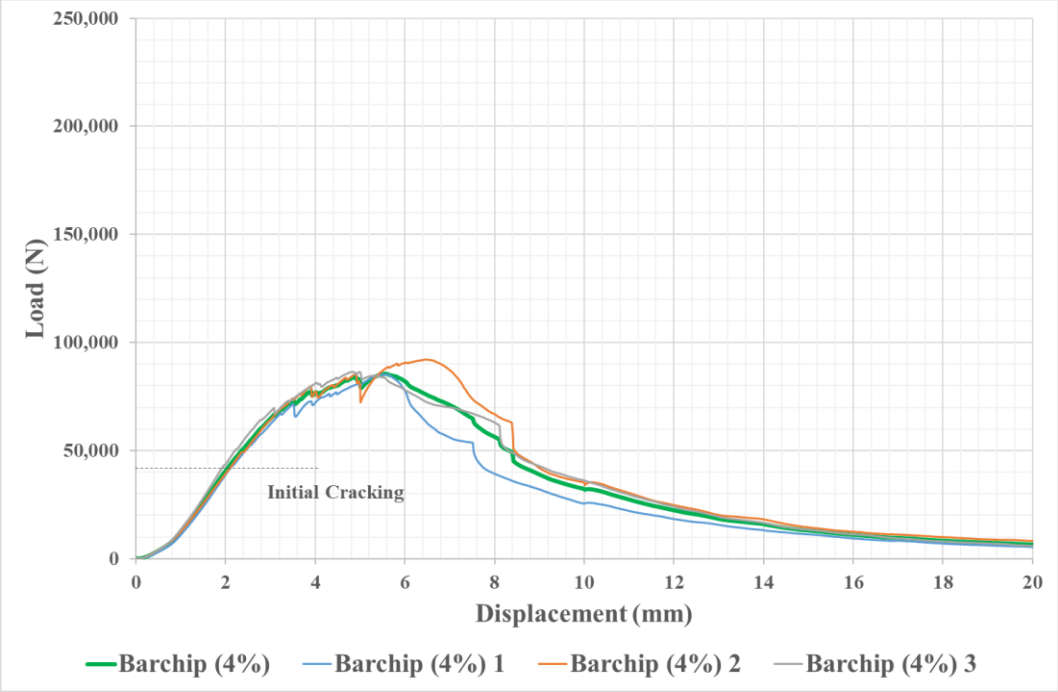

Figure A.2. Load-Deflection Curves of FRC with Barchip Fibers 4%

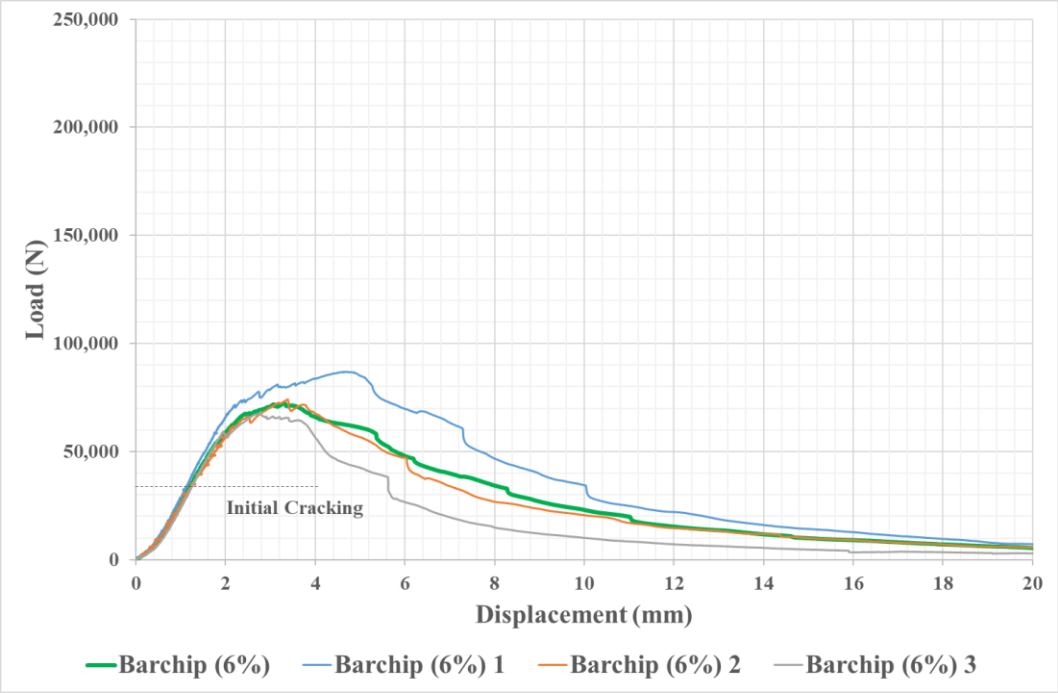

Figure A.3. Load-Deflection Curves of FRC with Barchip Fibers 6%

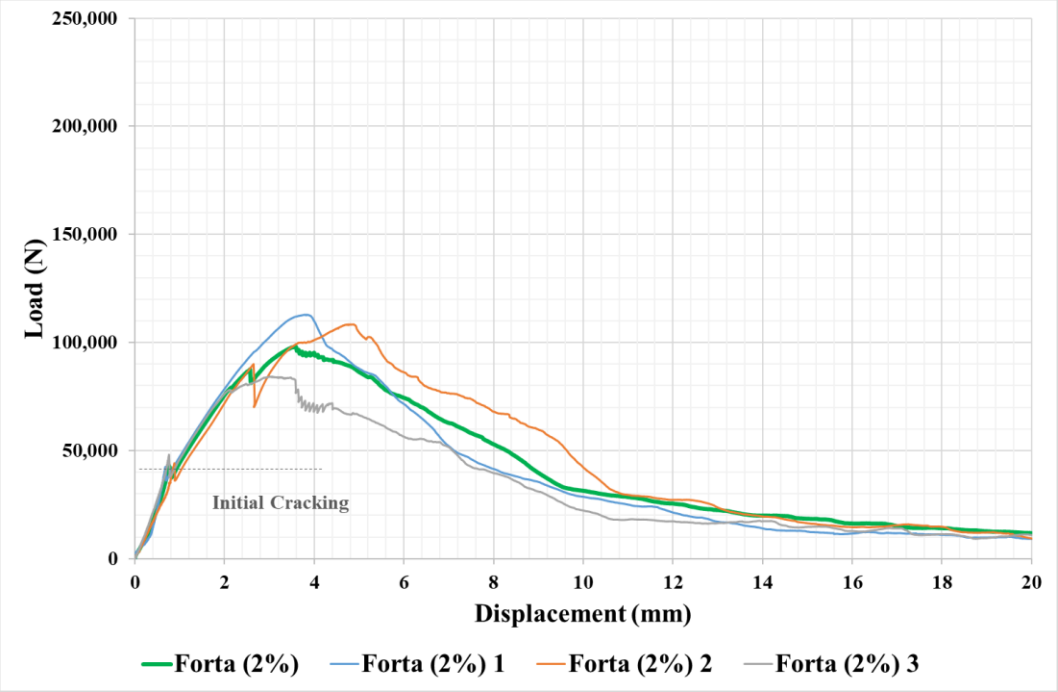

Figure A.4. Load-Deflection Curves of FRC with Forta Fibers 2%

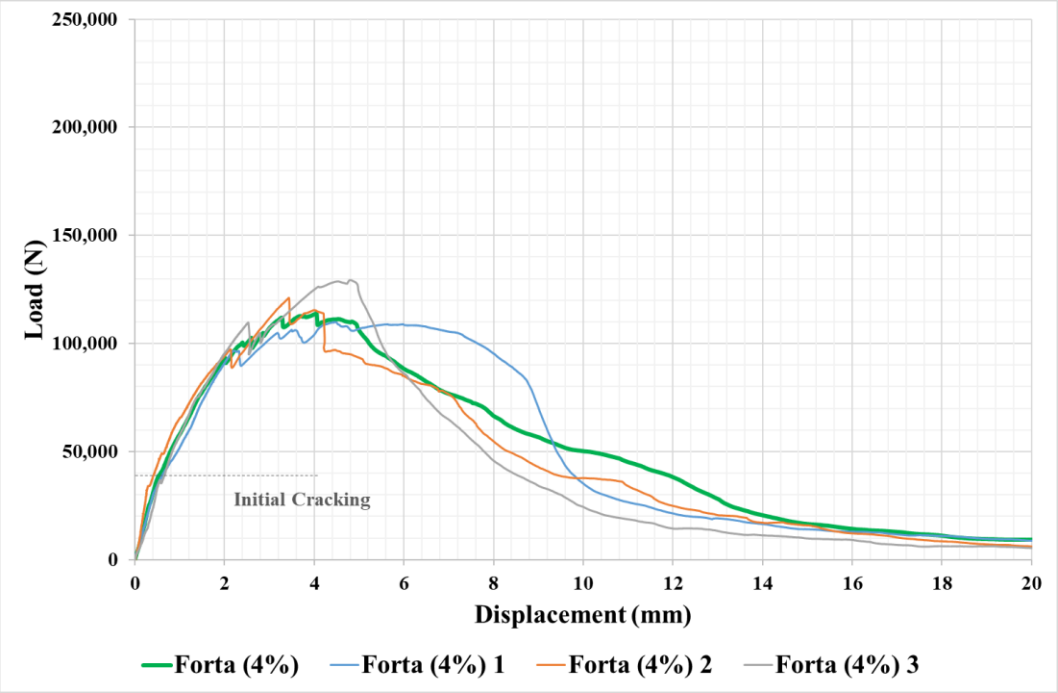

Figure A.5. Load-Deflection Curves of FRC with Forta Fibers 4%

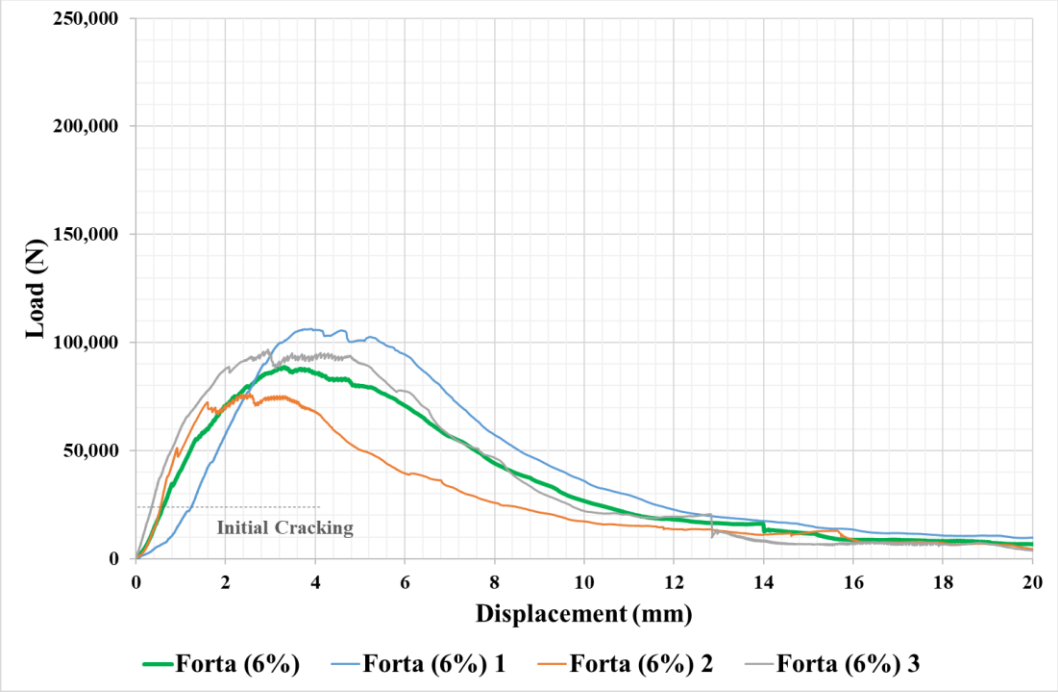

Figure A.6. Load-Deflection Curves of FRC with Forta Fibers 6%

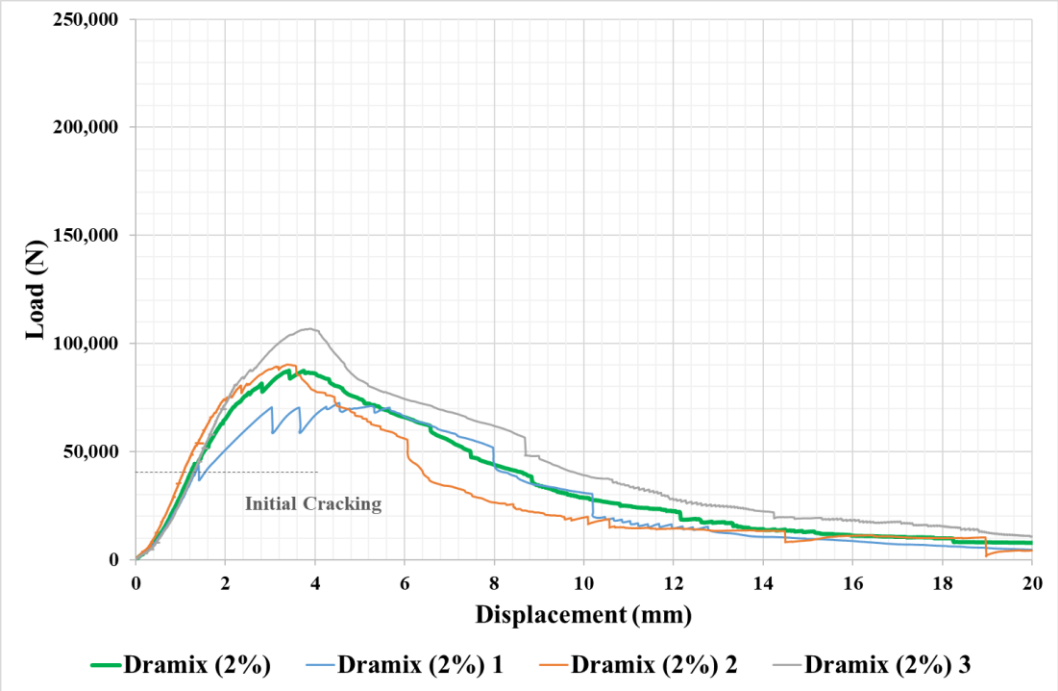

Figure A.7. Load-Deflection Curves of FRC with Dramix Fibers 2%

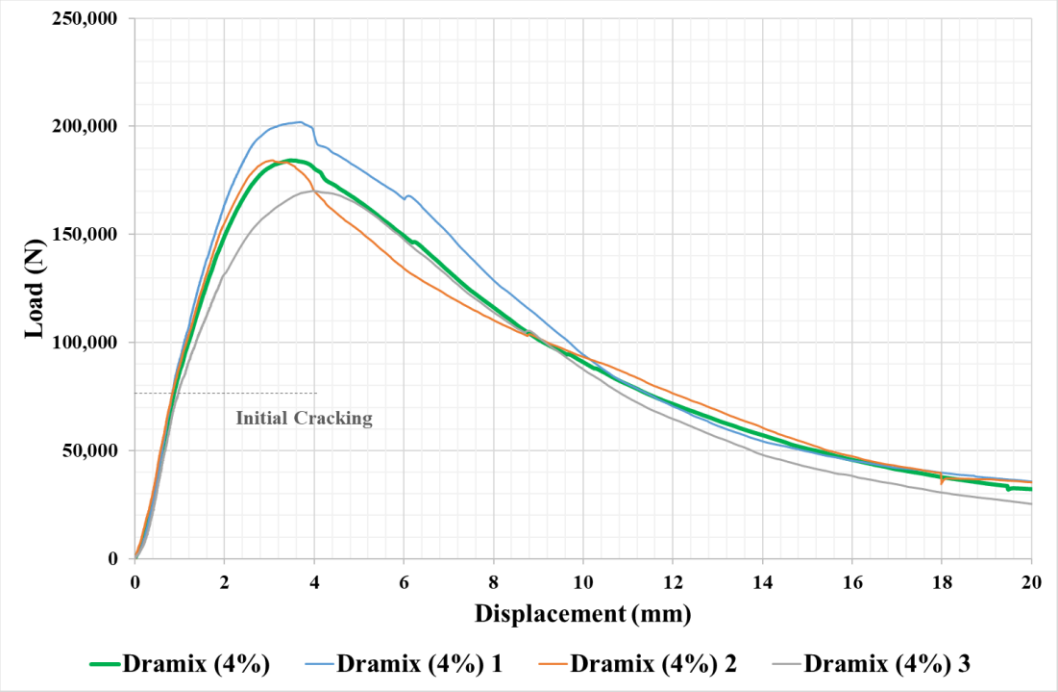

Figure A.8. Load-Deflection Curves of FRC with Dramix Fibers 4%

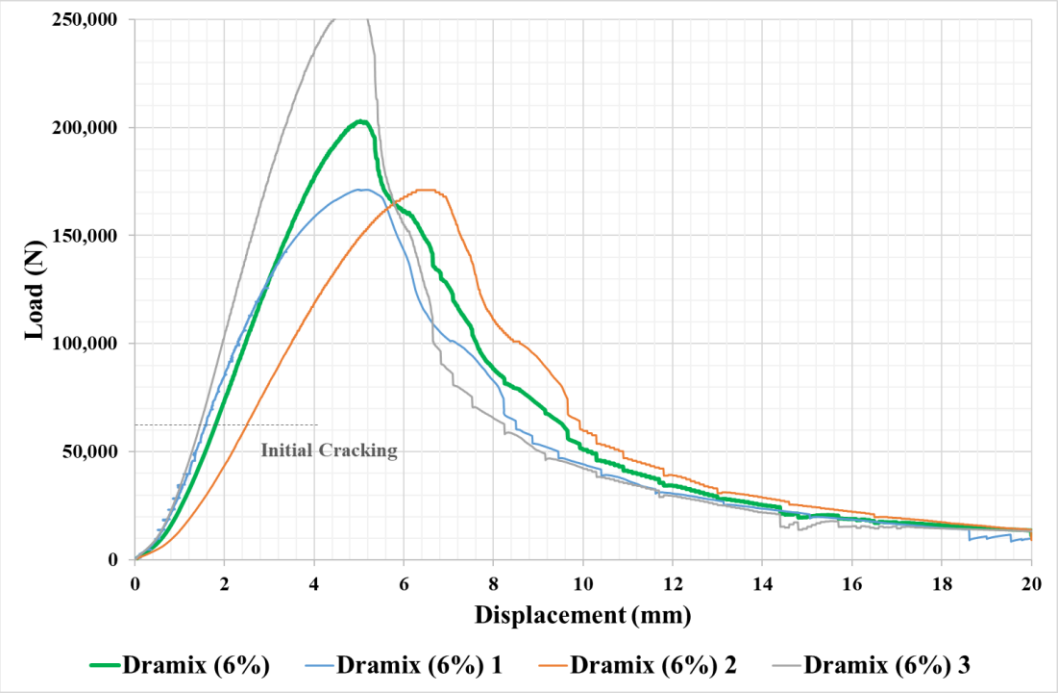

Figure A.9. Load-Deflection Curves of FRC with Dramix Fibers 6%

Energy-Deflection Curves

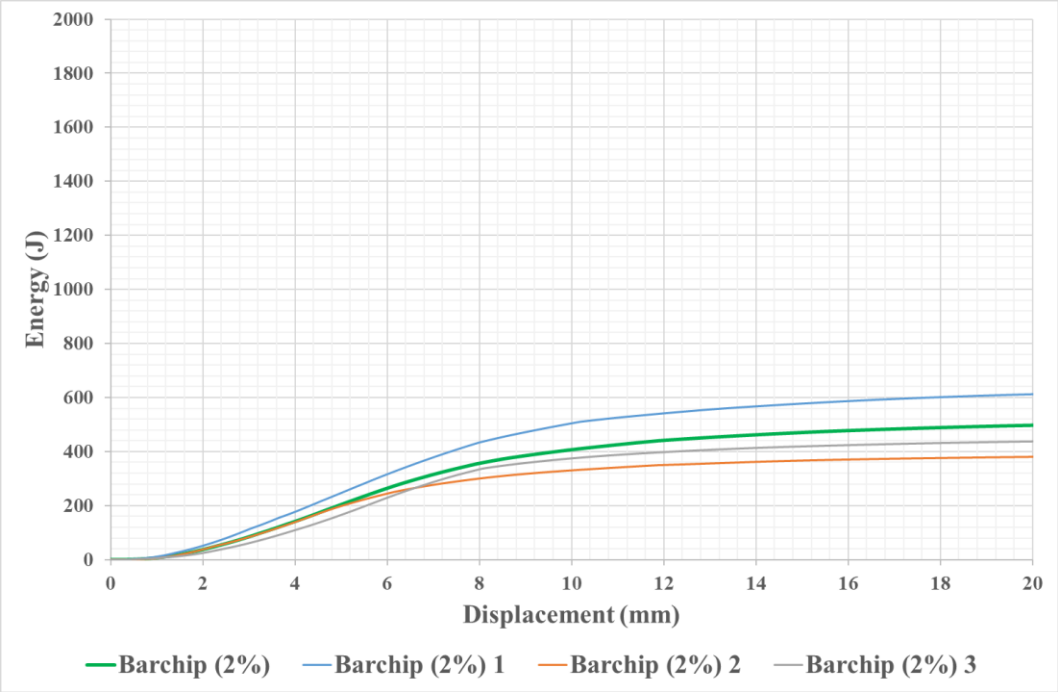

Figure A.10. Energy-Deflection Curves of FRC with Barchip Fibers 2%

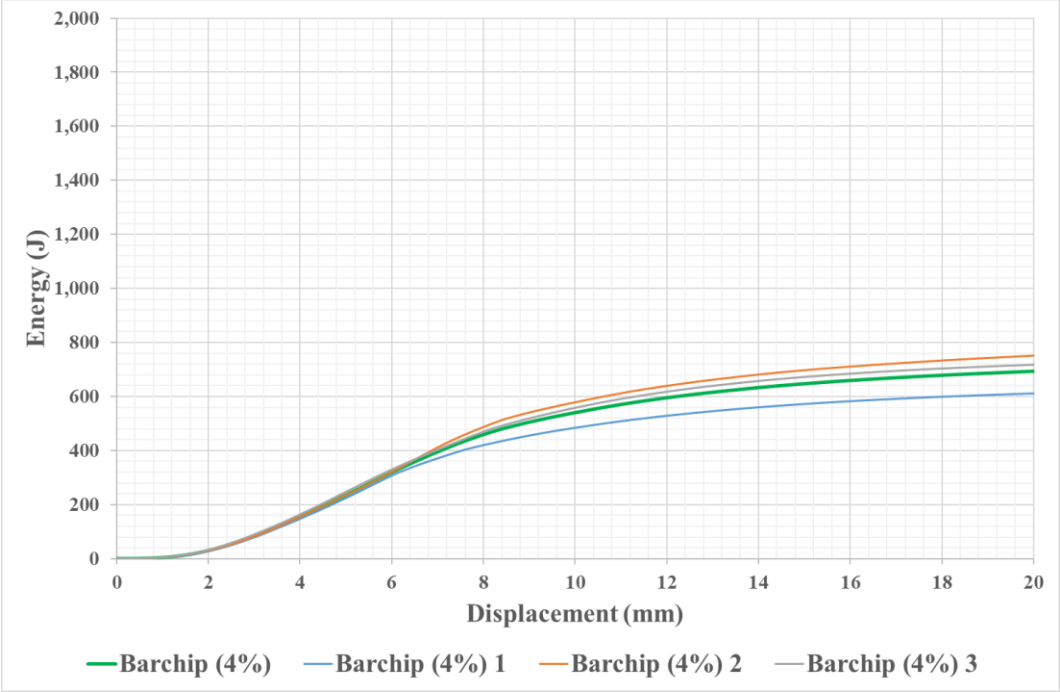

Figure A.11. Energy-Deflection Curves of FRC with Barchip Fibers 4%

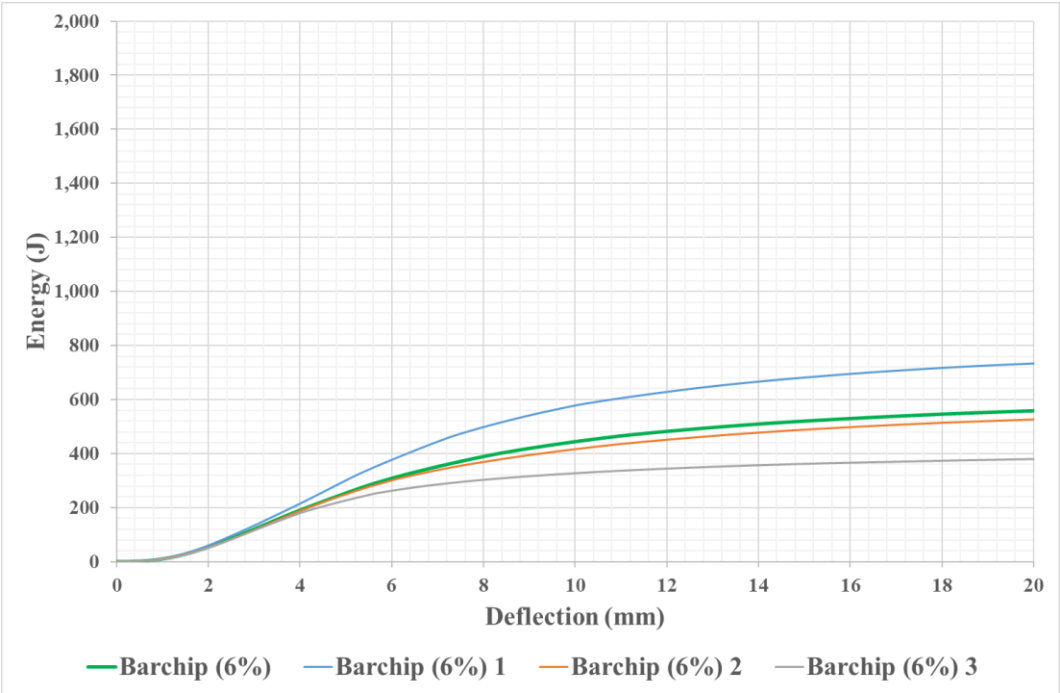

Figure A.12. Energy-Deflection Curves of FRC with Barchip Fibers 6%

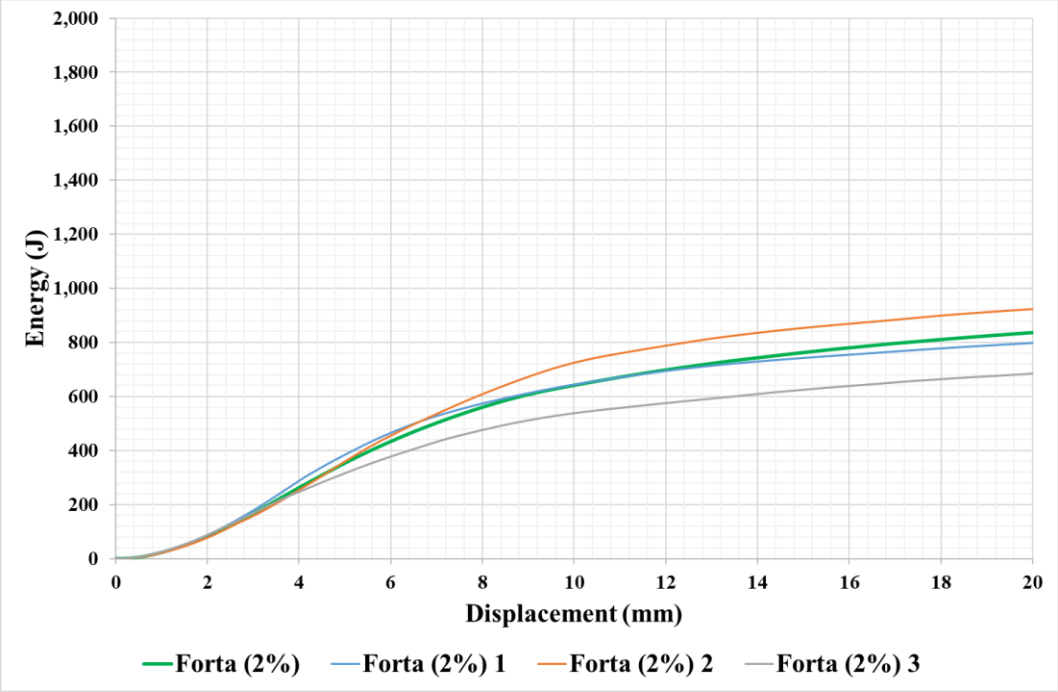

Figure A.13. Energy-Deflection Curves of FRC with Forta Fibers 2%

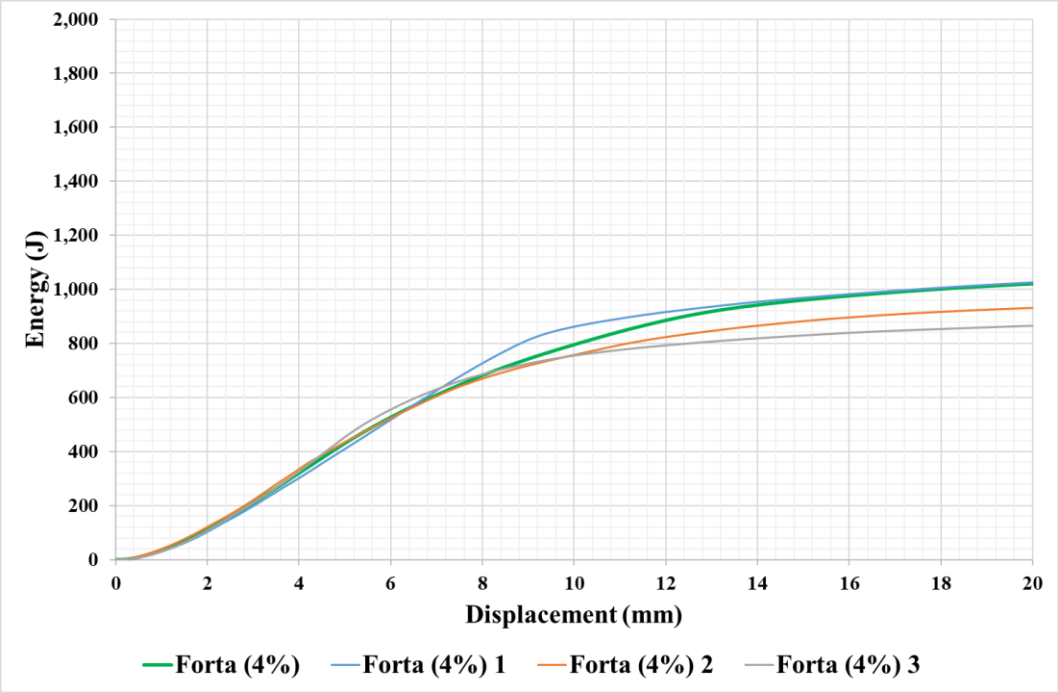

Figure A.14. Energy-Deflection Curves of FRC with Forta Fibers 4%

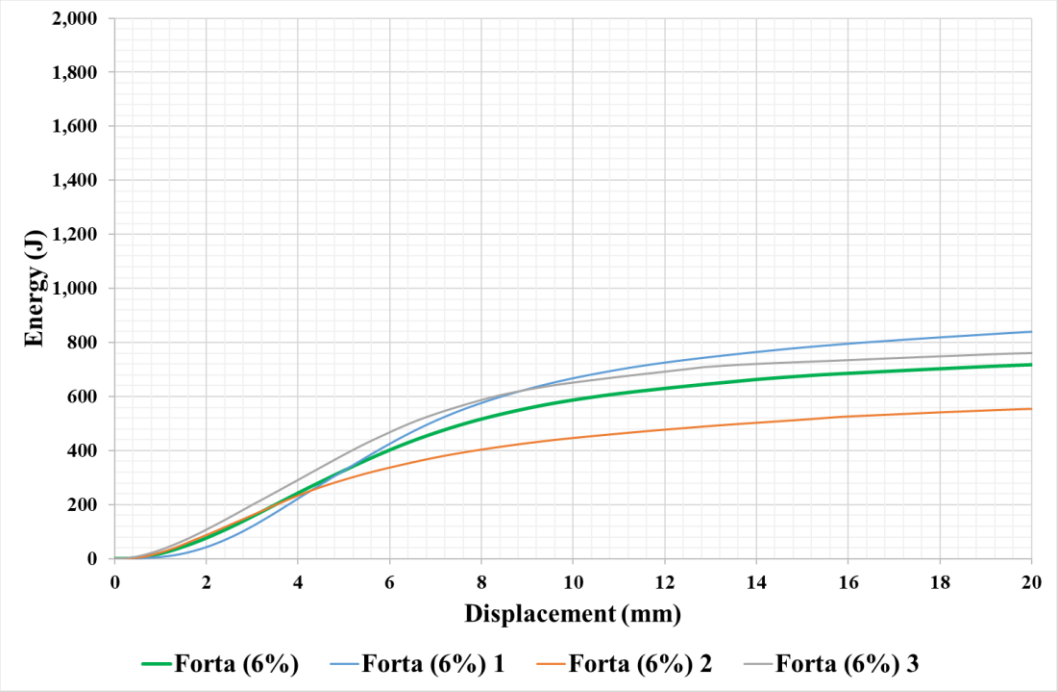

Figure A.15. Energy-Deflection Curves of FRC with Forta Fibers 6%

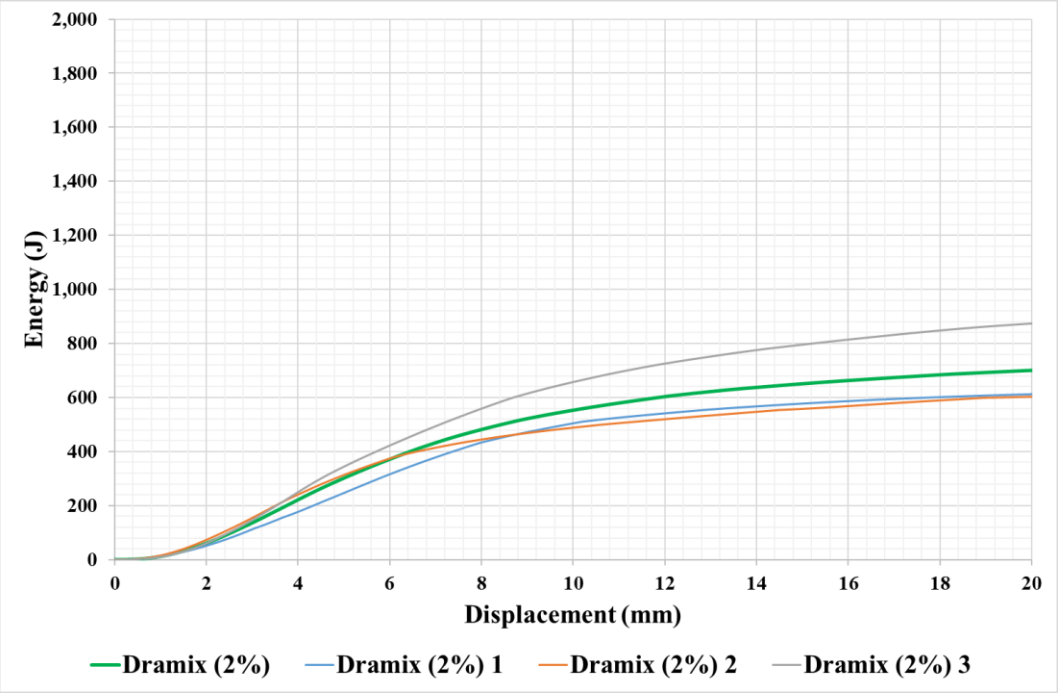

Figure A.16. Energy-Deflection Curves of FRC with Dramix Fibers 2%

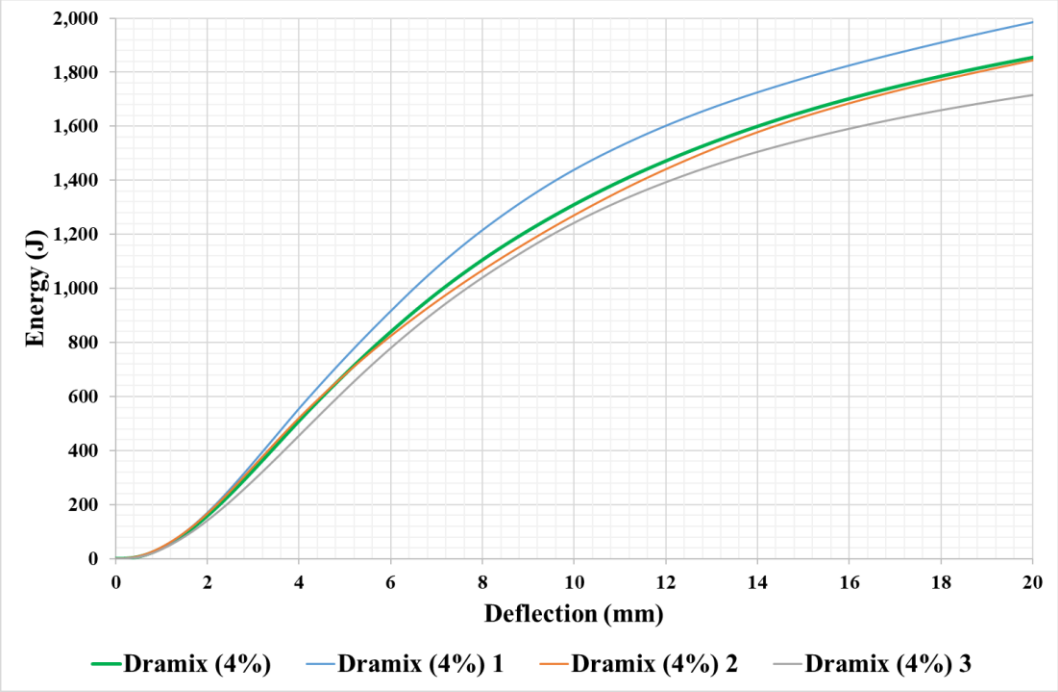

Figure A.17. Energy-Deflection Curves of FRC with Dramix Fibers 4%

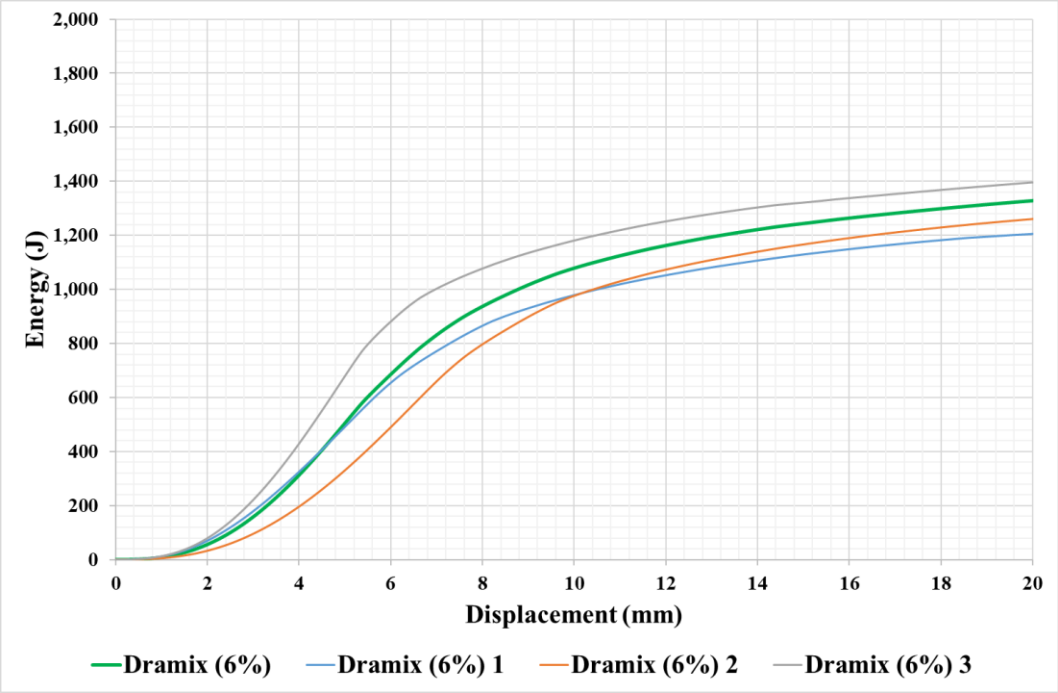

Figure A.18. Energy-Deflection Curves of FRC with Dramix Fibers 6%

B. Splitting Tensile Strength Test Curves

Load-Deflection Curves

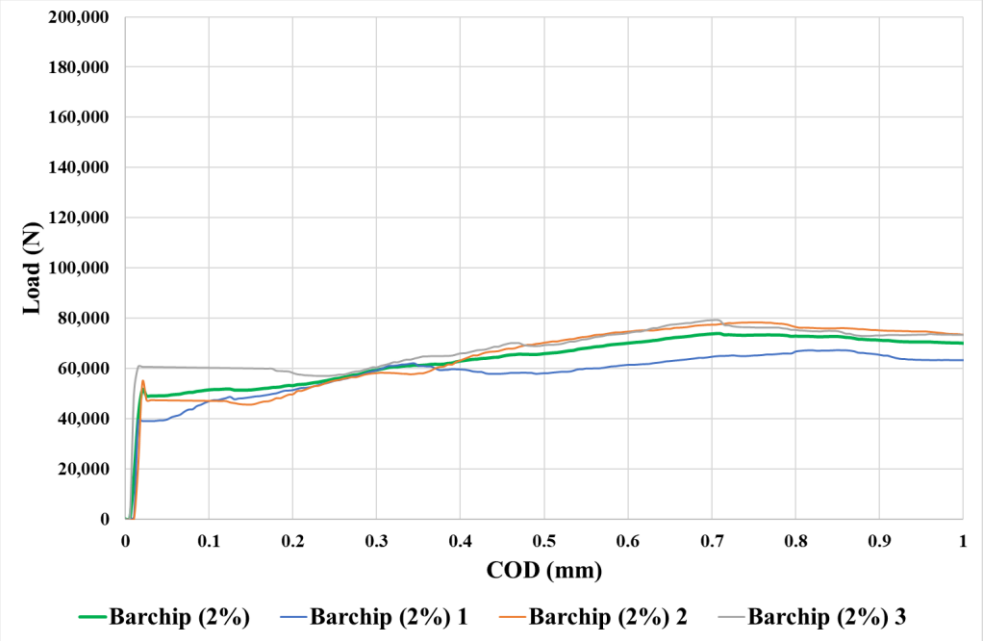

Figure A.19. Load-Deflection Curves of FRC with Barchip Fibers 2%

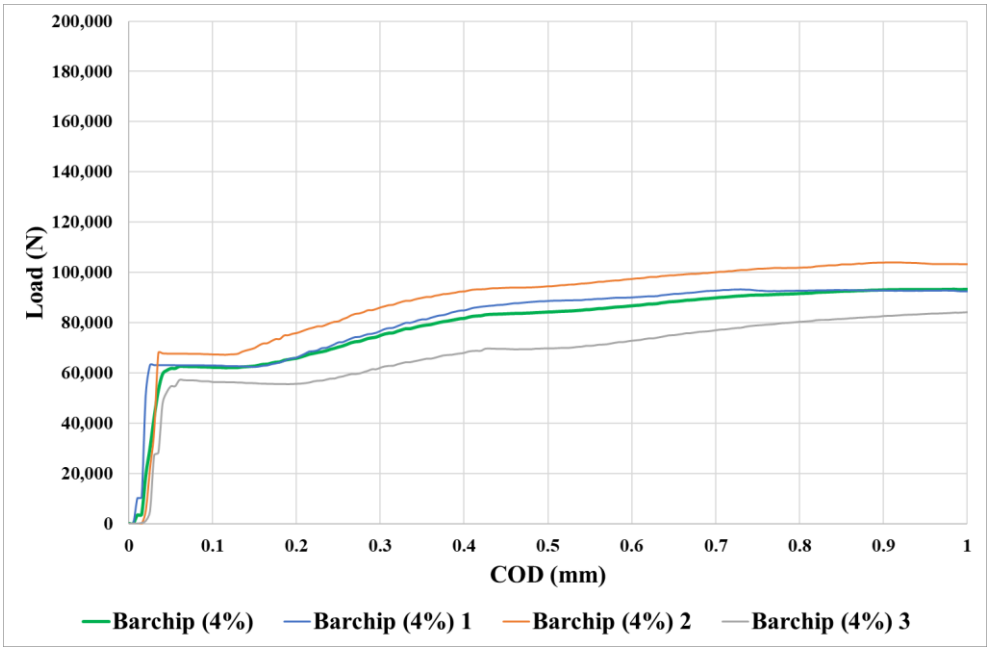

Figure A.20. Load-Deflection Curves of FRC with Barchip Fibers 4%

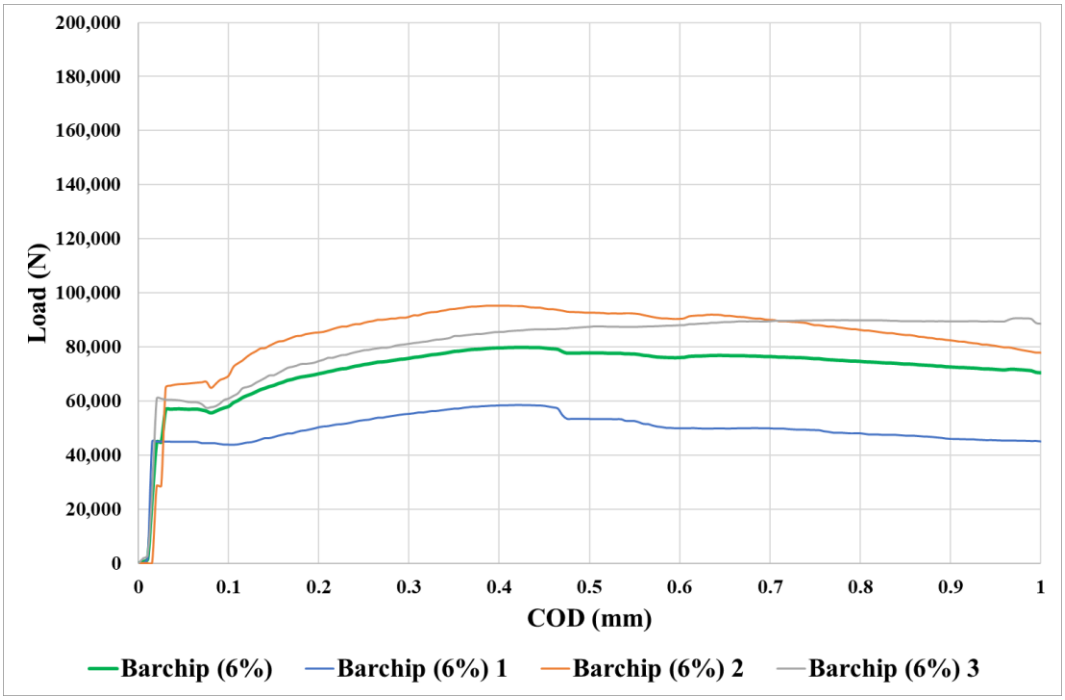

Figure A.21. Load-Deflection Curves of FRC with Barchip Fibers 6%

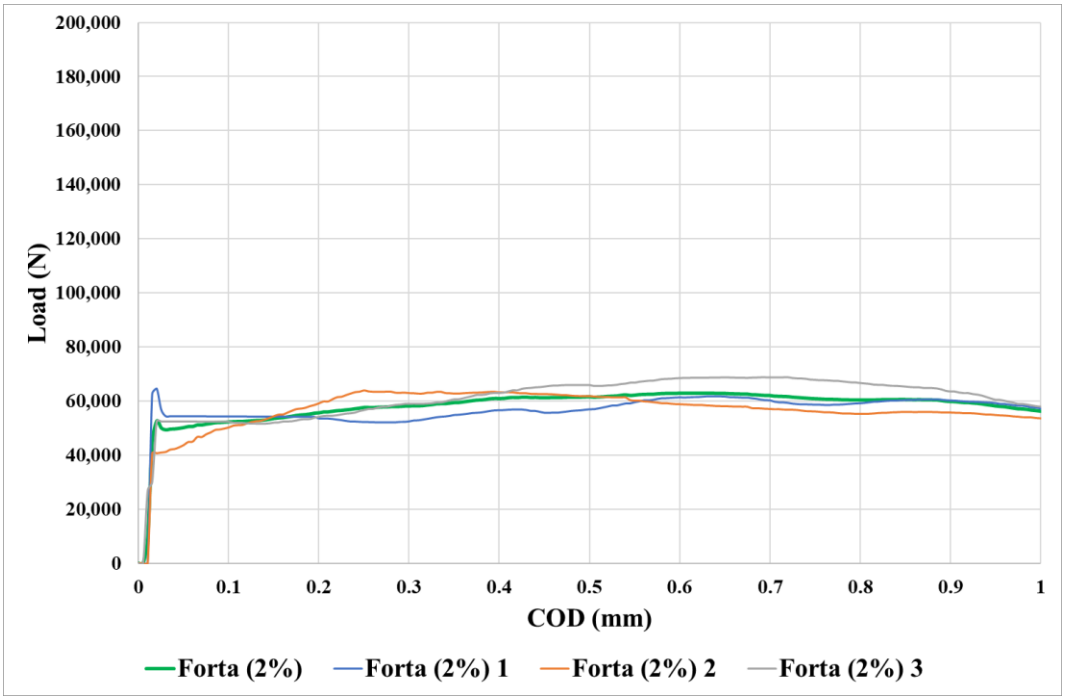

Figure A.22. Load-Deflection Curves of FRC with Forta Fibers 2%

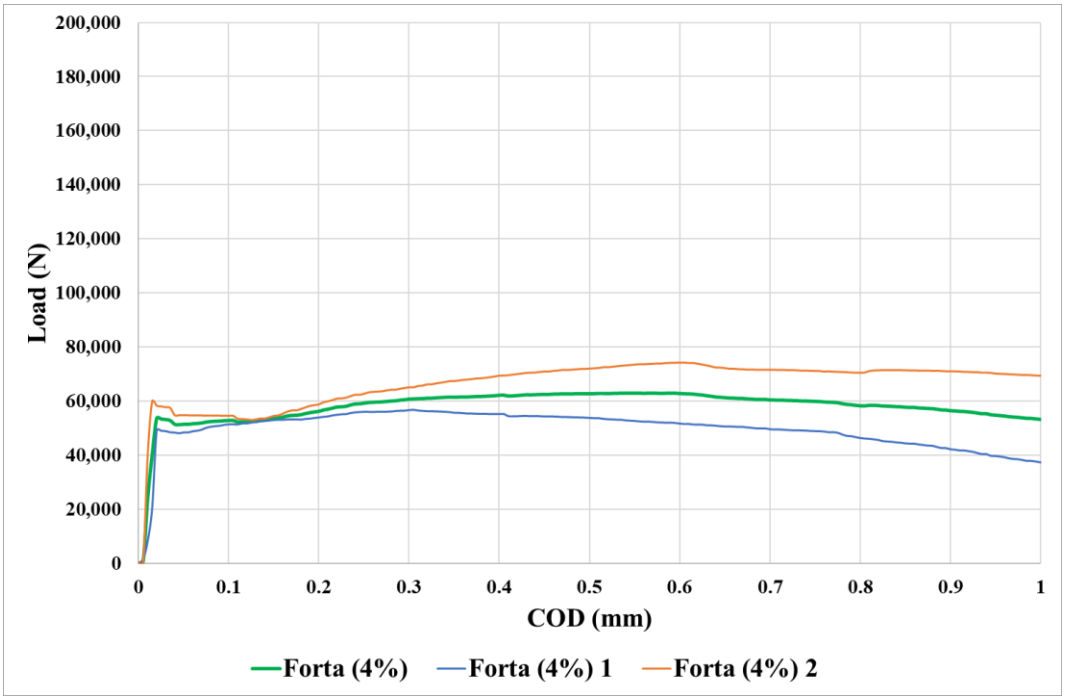

Figure A.23. Load-Deflection Curves of FRC with Forta Fibers 4%

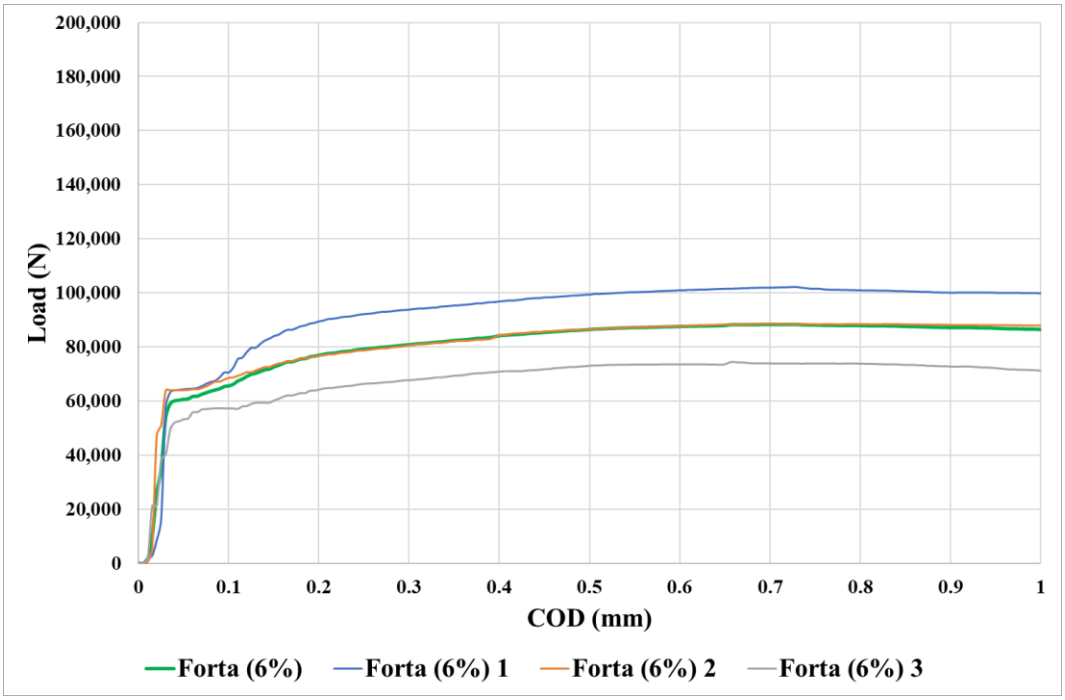

Figure A.24. Load-Deflection Curves of FRC with Forta Fibers 6%

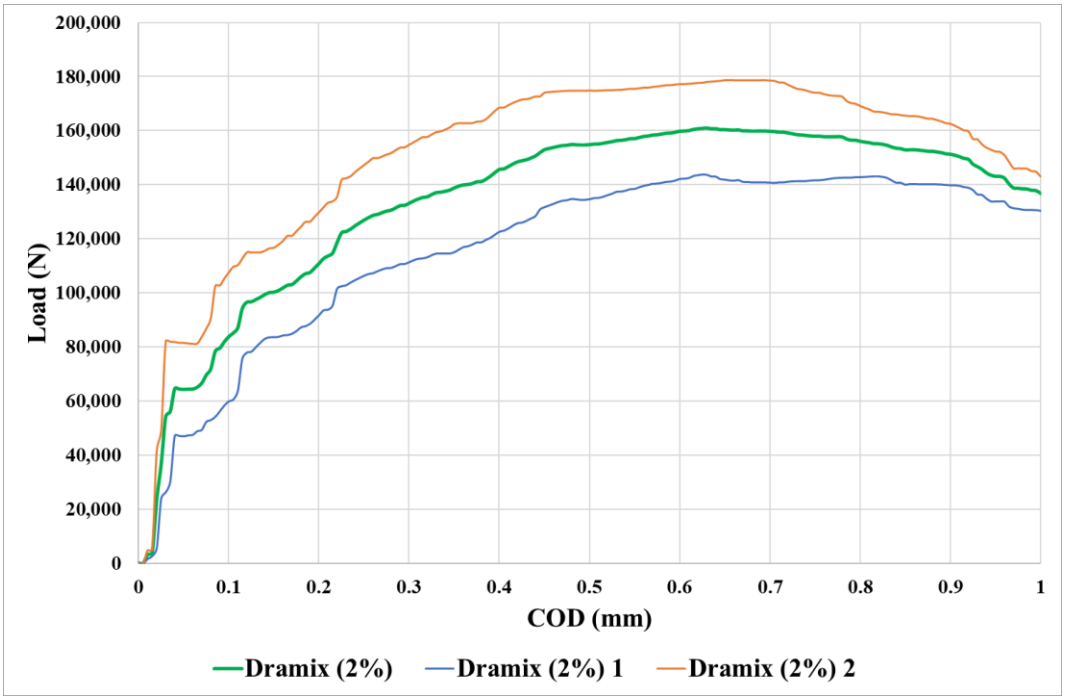

Figure A.25. Load-Deflection Curves of FRC with Dramix Fibers 2%

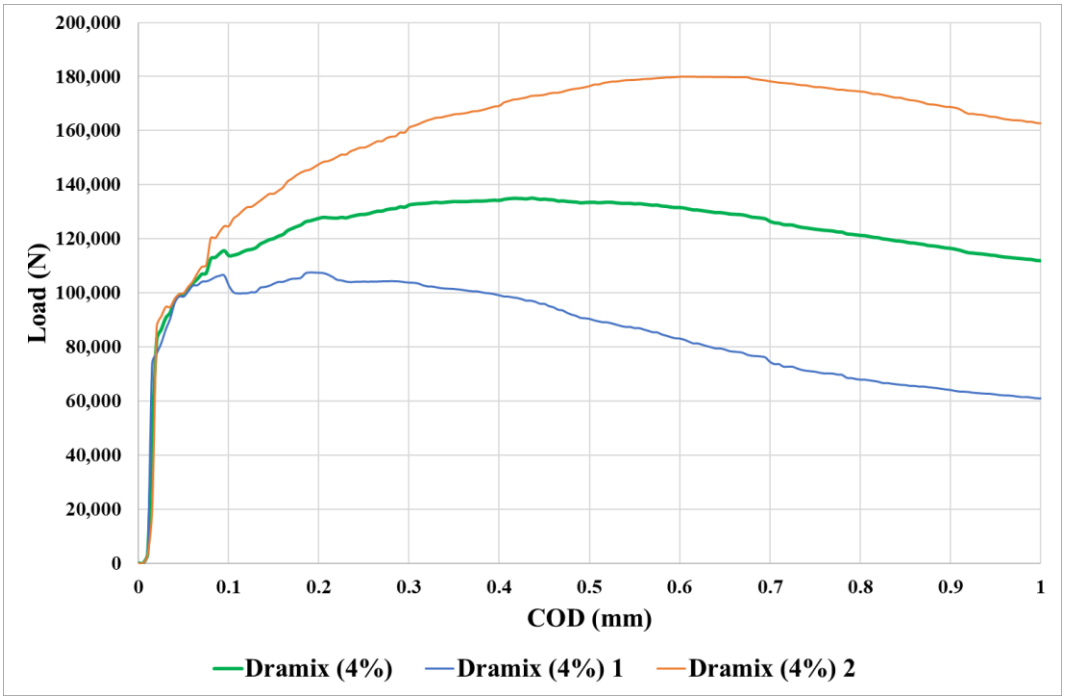

Figure A.26. Load-Deflection Curves of FRC with Dramix Fibers 4%

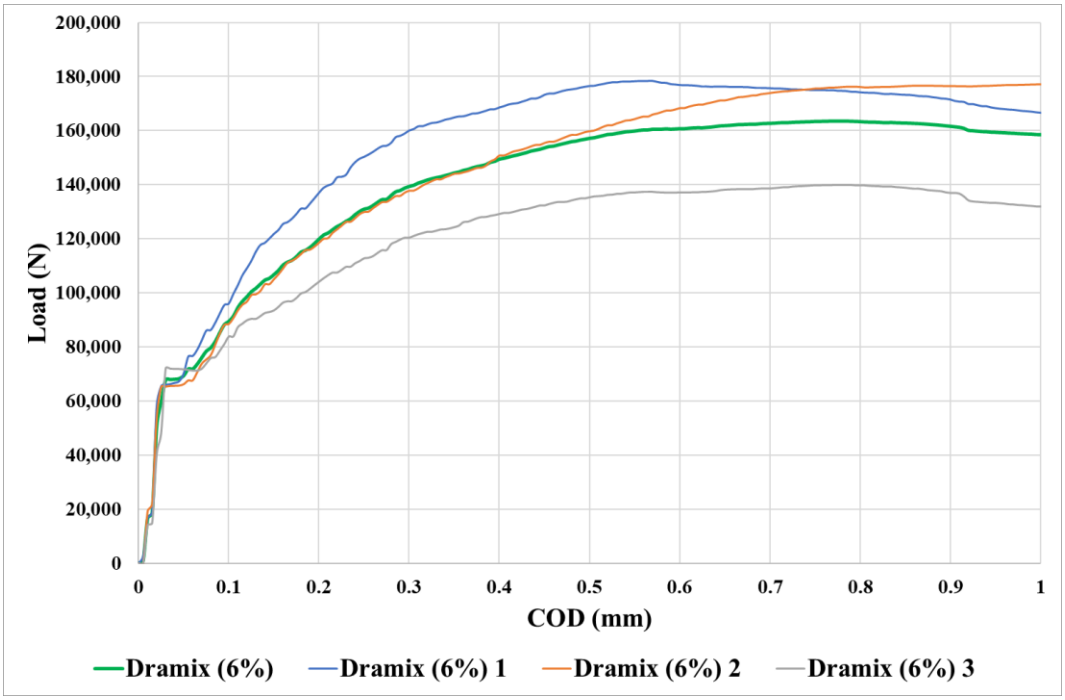

Figure A.27. Load-Deflection Curves of FRC with Dramix Fibers 6%

Load×COD-Deflection Curves

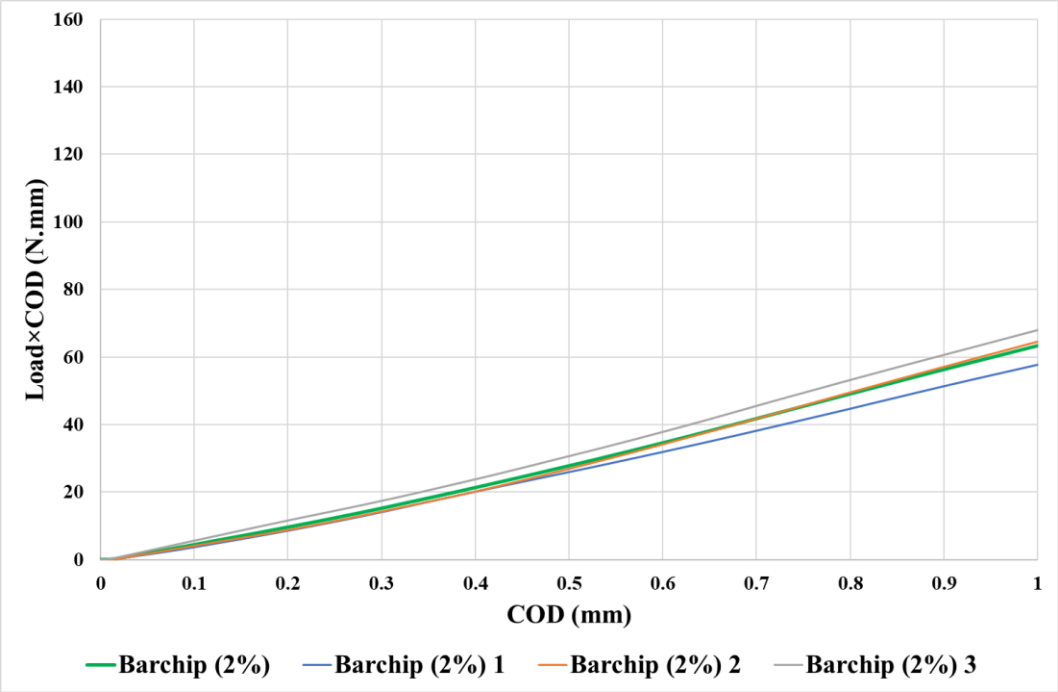

Figure A.28. Load×COD-Deflection Curves of FRC with Barchip Fibers 2%

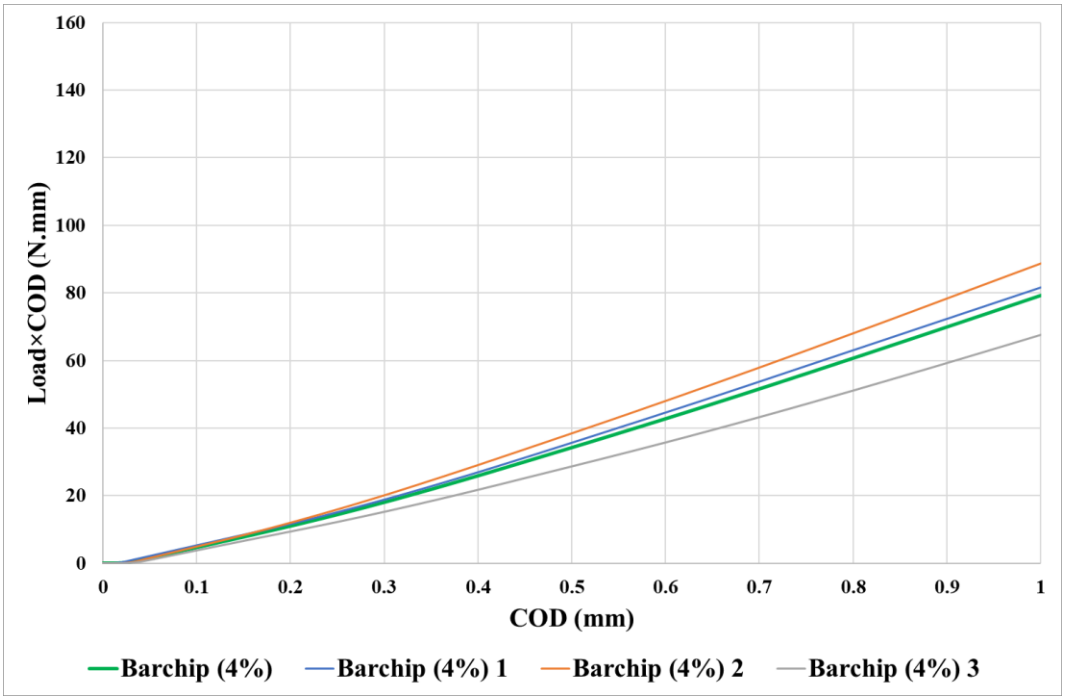

Figure A.29. Load×COD-Deflection Curves of FRC with Barchip Fibers 4%

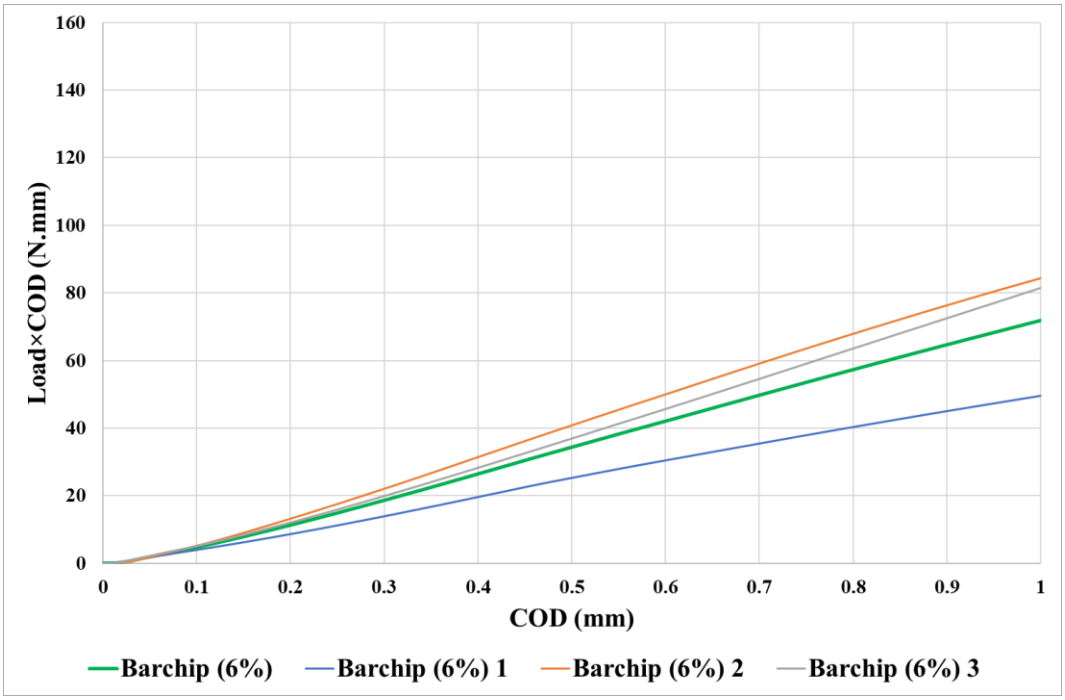

Figure A.30. Load×COD-Deflection Curves of FRC with Barchip Fibers 6%

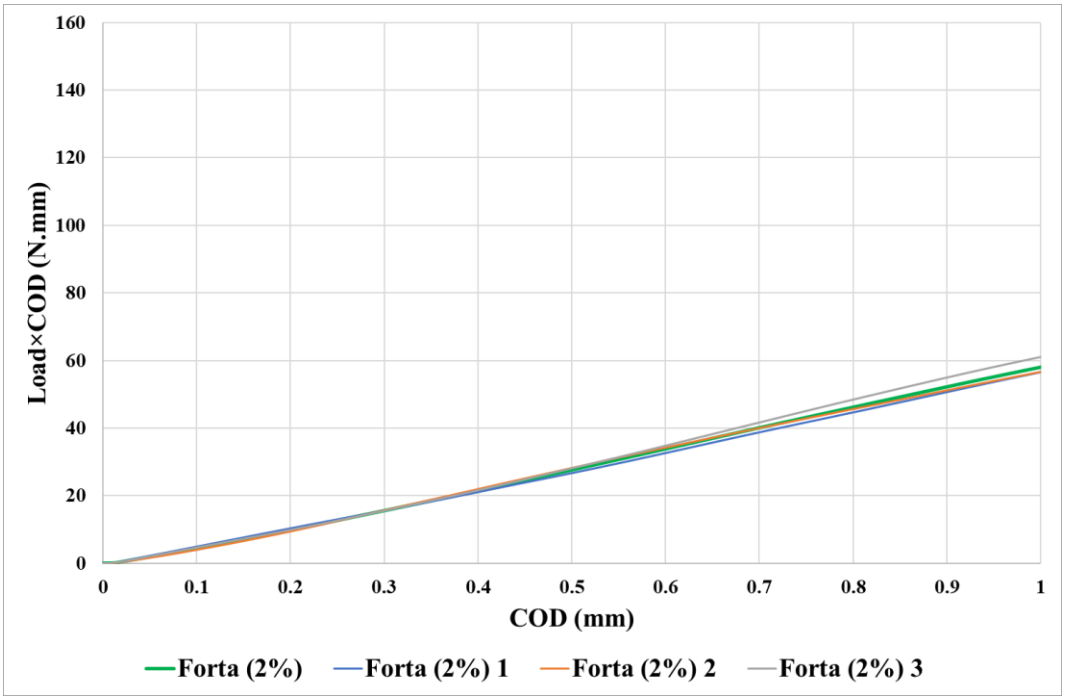

Figure A.31. Load×COD-Deflection Curves of FRC with Forta Fibers 2%

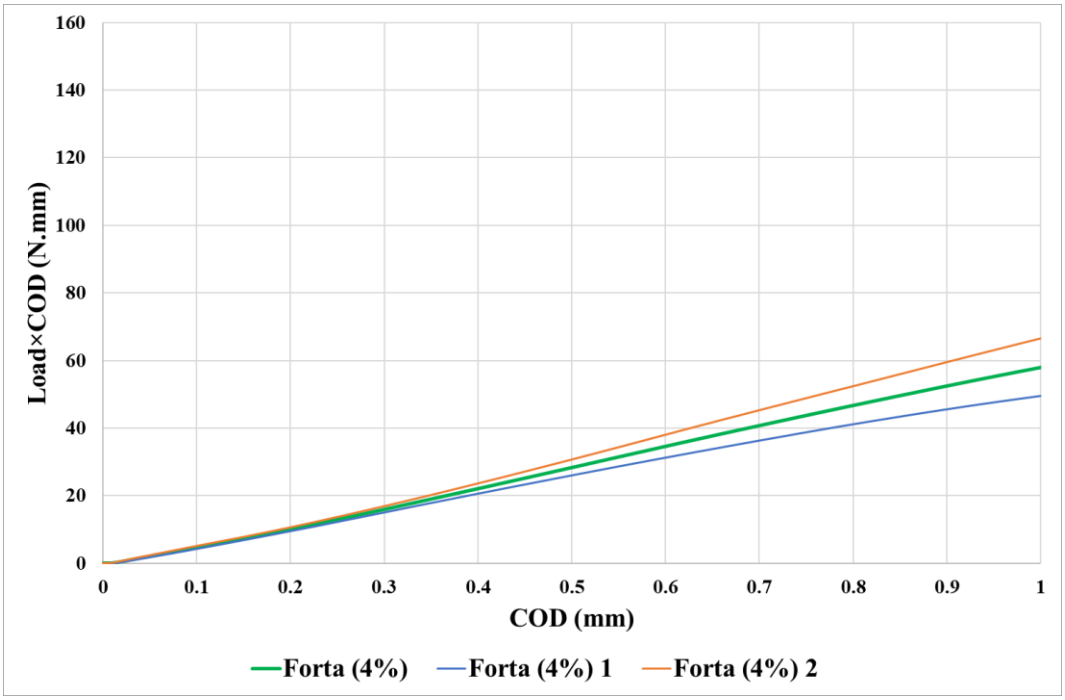

Figure A.32. Load×COD-Deflection Curves of FRC with Forta Fibers 4%

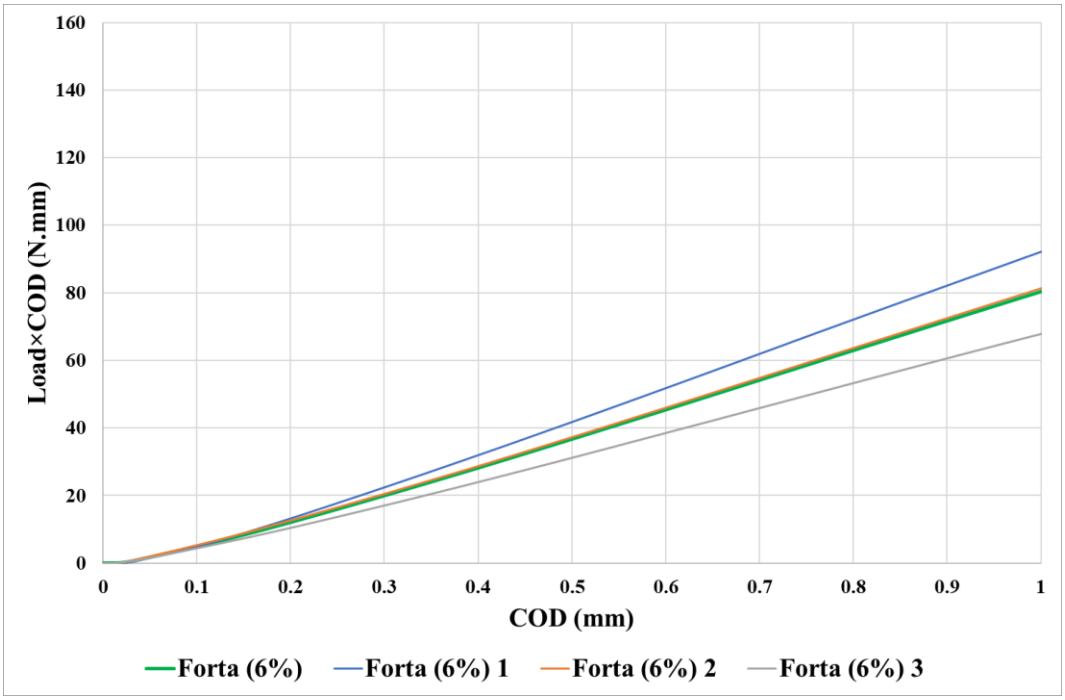

Figure A.33. Load×COD-Deflection Curves of FRC with Forta Fibers 6%

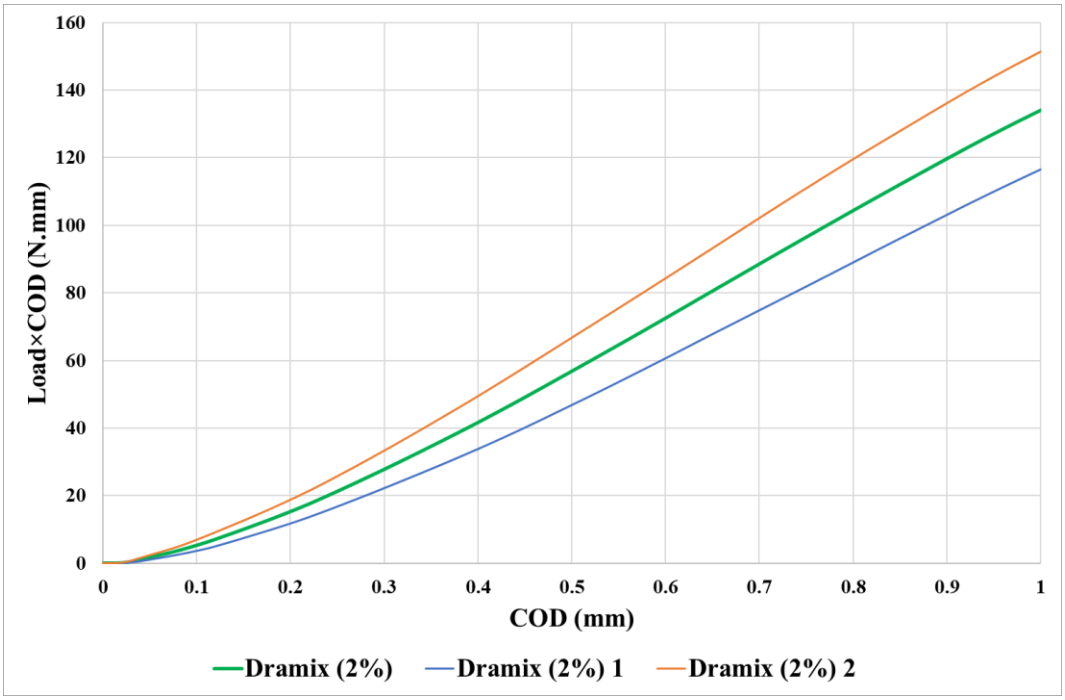

Figure A.34. Load×COD-Deflection Curves of FRC with Dramix Fibers 2%

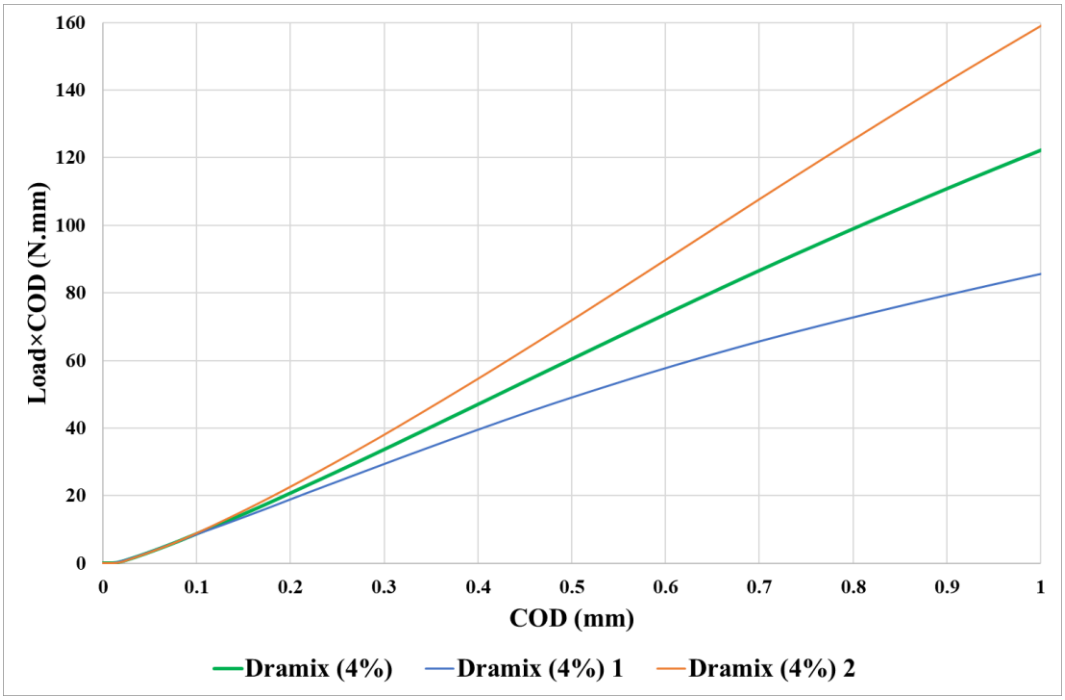

Figure A.35. Load×COD-Deflection Curves of FRC with Dramix Fibers 4%

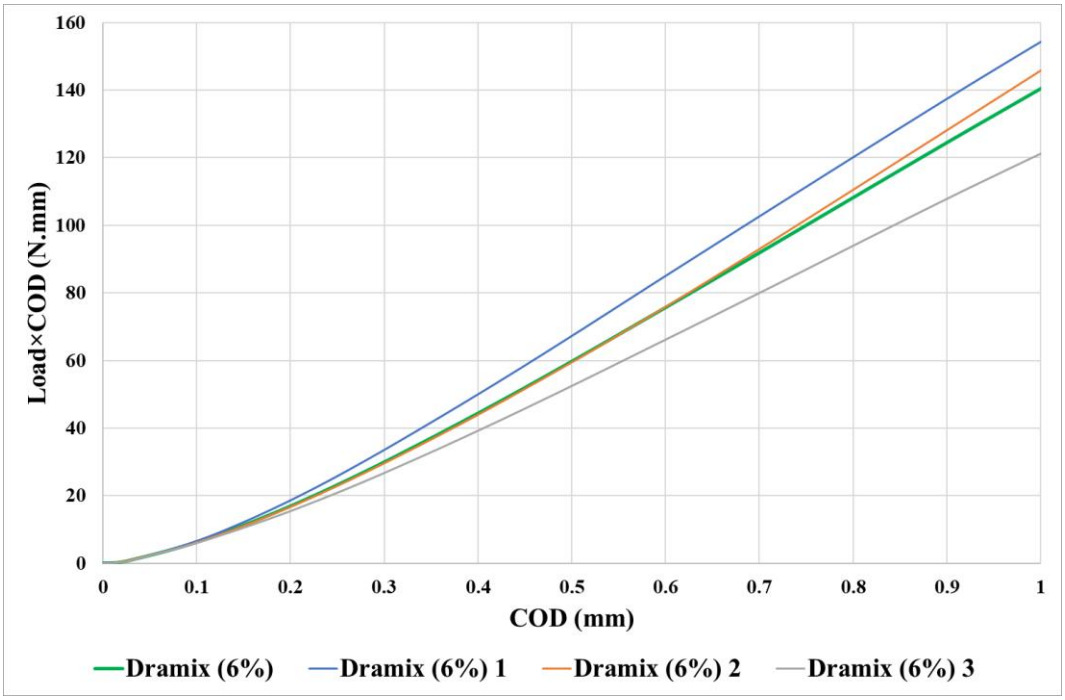

Figure A.36. Load×COD-Deflection Curves of FRC with Dramix Fibers 6%